POLITECNICO DI MILANO
School of Industrial and Information Engineering
Department of Energy

# Study And Evaluation of Direct Resistance Heating System in The Extrusion Heating Process

Master of Science in Electrical Engineering

Author: **Amin Ali Zadeh**

Student ID: 927284
Advisor: Prof. Roberto Sebastiano Faranda
Danieli Advisor: Eng. Matteo Gianinetti
Academic Year: 2021-2022

# Table of Contents

# Abstract

This thesis studies the possibility of using Direct Resistance Heating (DRH) process in hot extrusion instead of rapid gas-fired furnaces commonly used in the extrusion industry and also providing a comparison between these two heating systems.

Here within this work, DRH system working with both DC and AC power supplies has been analysed by using mathematical models and using analytical data for feasibility study and then using experimental data for validation of our implemented methodology.

In detail, this work investigates the feasibility of the DRH system for such applications by analyzing the electrical and thermal issues that might exist when designing such a system with both DC and AC power feeding concepts.

Performing a feasibility study from the electrical point of view (in both DC and AC feeding systems), simplified electrical equations of an equivalent circuit of a DRH system are used to produce meaningful results in terms of system limitations. From the thermal point of view, instead, the system limitations due to high operating temperatures as well as the thermal efficiency of the system have been studied by using the concept of heat transferring.

This study demonstrates that DRH system working with both DC and AC power feeding is not a practical solution for heating a workpiece (billet) in the extrusion process due to various limitations which have extensively been discussed in this work.

# Sommario

Questa tesi studia la possibilità di utilizzare il processo di riscaldamento a resistenza diretta (DRH) nell'estrusione a caldo al posto dei forni a gas rapidi comunemente utilizzati nell'industria dell'estrusione e fornisce anche un confronto tra questi due sistemi di riscaldamento.

In questo lavoro, il sistema DRH funzionante con alimentatori CC e CA è stato analizzato utilizzando modelli matematici e utilizzando dati analitici per lo studio di fattibilità e quindi utilizzando dati sperimentali per la convalida della nostra metodologia implementata.

In dettaglio, questo lavoro indaga la fattibilità del sistema DRH per tali applicazioni analizzando i problemi elettrici e termici che potrebbero esistere durante la progettazione di un tale sistema con concetti di alimentazione sia CC che CA.

Effettuando uno studio di fattibilità dal punto di vista elettrico (sia nei sistemi di alimentazione DC che AC), si utilizzano equazioni elettriche semplificate di un circuito equivalente di un sistema DRH per produrre risultati significativi in termini di limitazioni del sistema. Dal punto di vista termico, invece, sono stati studiati i limiti del sistema dovuti alle elevate temperature di esercizio nonché l'efficienza termica del sistema utilizzando il concetto di scambio termico.

Questo studio dimostra che il sistema DRH funzionante con alimentazione sia CC che CA non è una soluzione pratica per riscaldare un pezzo (billetta) nel processo di estrusione a causa di varie limitazioni che sono state ampiamente discusse in questo lavor.

# Chapter 1

# 1 Introduction

The extrusion process involves forcing base metal through a pre-shaped die to create objects with specific shapes and profiles. As the metal moves through the die, the form of the metal will change based on the die's shape. There are different types of extrusion processes including hot and cold extrusion in which both can operate in the form of direct and indirect extrusion.

In the hot extrusion process, there is a need for a heating system before transferring the billets to the press machine for the extrusion process. There are several heating methods in industry application, for example, Gas-fried furnace, Induction furnace, and Direct Resistance Heating, but the most common method by considering the diameter and physical characteristics of the material is the combination of rapid heating gas-fired and an induction furnace.

## 1.1 Introduction

Extrusion is a metal forming process that is widely used in industry and daily life equipment. The process of Extrusion is used to create a fixed cross-sectional profile object. A material is pushed through a die of the desired cross-section. These fixed cross-sectional profile extruded parts are called "Extrudates" and pushed out using either a mechanical or hydraulic press.

The most generally extruded materials are Aluminum, Copper, Steel, Magnesium, and Lead. Plastics and ceramics are also extruded extensively but not discussed in this thesis.

## 1.2 Historical Development of Extrusion

The world's first extruder was built in 1795 by Joseph Bramah, and a manual piston-type extruder was used to make seamless lead pipes. This process involved two steps, first in which metal was preheated and the second step was to force the heated metal through a die through a plunger that was hand driven [1].

Joseph Bramah is also developed the first hydraulic press for Thomas Burr in 1820. This hydraulic press formed the first lead pipes that revolutionized the metal forming industry.

The modern hot extrusion process was developed in 1894 by Alexander Dick. This process allowed non-ferrous alloys to be extruded.

Nowadays, the extrusion of metals is pressed by a stem at high pressure through the die to form the desired shape, to one or more lengths. The first significant achievement was obtained in the semifinished product industry in the twentieth century. The process was used mainly to produce bar, wire, tubes, and sections in aluminum alloys and copper alloys [2].

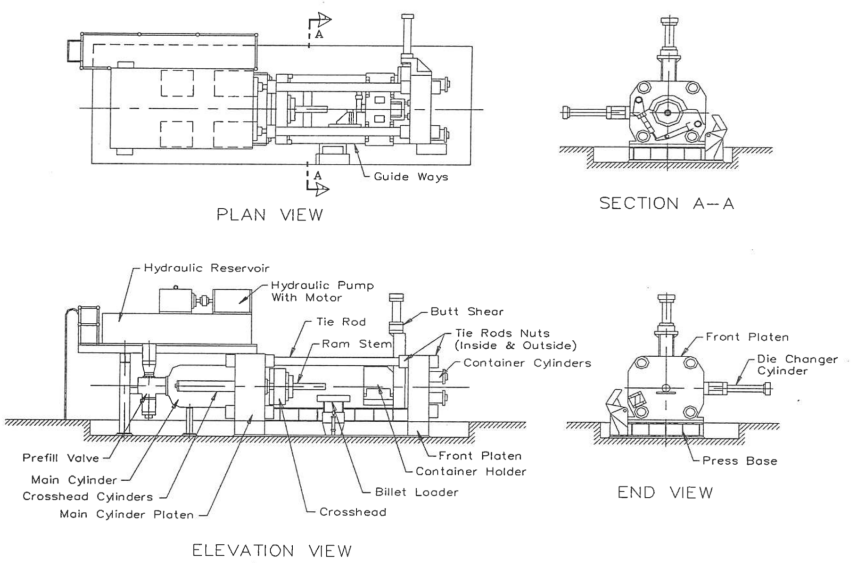


Figure 1.1 Extrusion press machine schematic

## 1.3 Process

The extrusion process starts with putting the billet into the container in the press machine. A dummy block is located behind it and pushes the billet through the die. After finishing the process, the container opens a short distance so that the discard can be separated from the die and extruded by a shear blade. The extrusion can then be pulled from the die. The container and the stem (with a loose dummy block), and the fixed dummy block are returned to the starting position [2].

While the core principles of the extrusion process are the same, we use two main classifications of the metal extrusion to achieve different product profiles.

- hot extrusion (when the billet is heated up to the certain temperature);

- cold extrusion (when extrusion is carried out at room temperature);

There is different equipment available for extrusion that depends on the die angle, reduction in cross-section, extrusion speed, billet temperature and lubrication all affect the extrusion pressure. The main extrusion equipment can be categorized and subdivided into the following.

- Direct Extrusion;
- Indirect Extrusion;

### 1.3.1 Direct Extrusion

Direct Extrusion is the most standard type of extrusion. In Direct Extrusion, a stem, generally with a dummy block in front, pushes the billet in a fixed container through the die (tool of the desired shape). Relative movement takes place between the container and the billet [3].

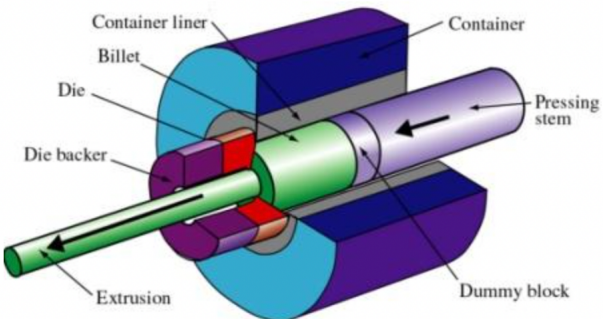


Figure 1.2 Direct Extrusion

### 1.3.2 Indirect Extrusion

In contrast, in Indirect Extrusion, the die is in front of a hollow stem and pushed against the billet by the forward movement of the container closed at the back. Since no relative motion, friction between the billet and chamber is eliminated and the required force is lower.

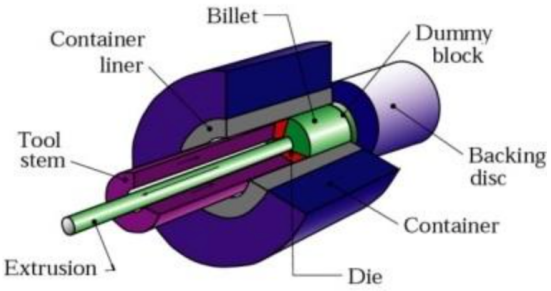


Figure 1.13 Indirect Extrusion

## 1.4 Extrusion Line Heating Systems

Today, in the extrusion process billets are usually heated to the desired operating temperature by induction or rapid-heating gas-fired furnaces. These two furnace types are used because they are best suited to meet the requirements of temperature control, flexibility, floor space, and so on of a billet-heating furnace in a modern extrusion plant. However, for a specific diameter and material, the direct resistance heating is also can be used.

### 1.4.1 Induction Furnaces

Induction heating is commonly used in various industrial applications such as melting, preheating, heat treatment, welding, and brazing. And it is due to its advantageous as compared to other traditional heating techniques such as resistance heating, flame heating, and furnaces because of its properties like the clean source of energy, fast, consistent heating, and low energy losses [5].

In the induction heating process, the alternative current passes through the primary coil and generates an alternating electromagnetic field Figure 1.4 [6]. The unique characteristic of induction heating is that the energy is directly released within the workpiece without affecting different neighbor elements due to the non-contact nature of heat transfer.

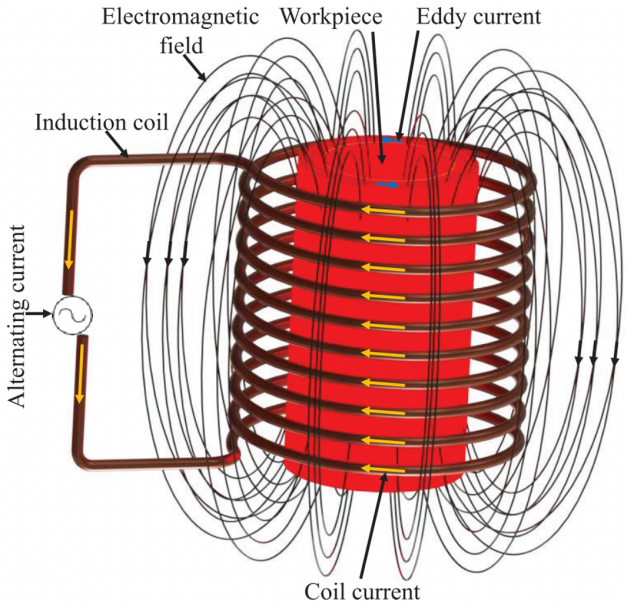


Figure 1.4 Typical induction heating principle

In Induction heating system (IH), the electromagnetic field lines run parallel to the billet axis in the middle of the billet (relative to the length) within the directly heated peripheral layer of thickness, $\delta$. At the end of the billet, the field lines can be subjected to a change in direction toward the billet edge or the billet core, depending on the size of the extension of the coil over the end of the billet.

Only a specific extension length of the coil guarantees a homogeneous field and temperature profile over the billet length. This optimal coil extension varies with the billet material and the diameter, as well as the energy input. If the coil extension is below the optimum, the field is weakened, resulting in a lower temperature at the end of the billet. The reverse effect occurs if the optimal coil extension is exceeded. This produces a field concentration and thus overheating at the billet end relative to the billet central line, Figure 1.5 [7].

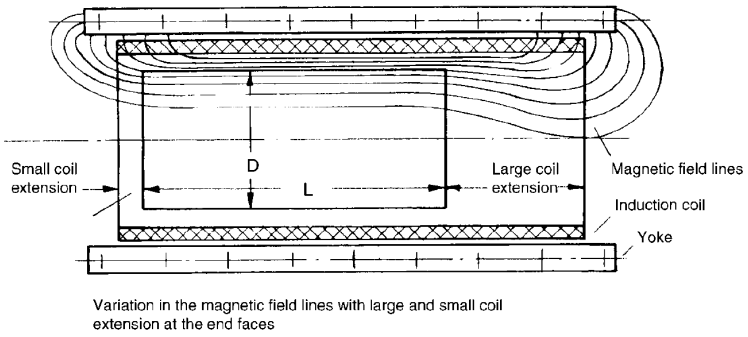


Figure 1.5 Distribution in the electromagnetic field line in the induction coil

These electromagnetic fields introduce the heat, that is produced uniformly within the billet in a layer over the full circumference, referred to as the penetration thickness, $\delta$ ,Figure 1.6 [8].

In Figure 1.7, the upper right section shows the produced heat by IH at the beginning of the process, which can be considered penetration thickness $\delta$. And then, due to thermal conductivity heat will transfer to the center of the billet.

The penetration thickness $\delta$ defines the thickness of the peripheral layer in which approximately 87% (see chapter 3) of the energy transferred to the billet is converted to heat. The thickness of this peripheral layer, which depends on the electrical and magnetic material properties of the billet as well as the frequency of the power supply [1].

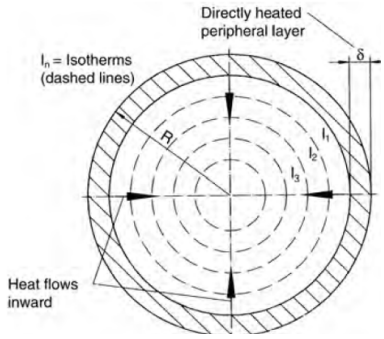


Figure 1.6 Penetration thickness

Figure 1.7 Development of heat in the billet by induction heating

In the billet, heat transfers by conduction into the core region from the peripheral layer, where the induced current flow causes heating. However, due to this heat conduction, there is thus a temperature difference between the billet surface and the billet core that develops from zero to a specific value and remains practically constant up to the end of the heating of the peripheral layer, Figure 1.8 [7] [8].

The magnitude of this temperature difference depends on the thermal conductivity of the material, the diameter of the billet, and the specific energy input. Because the surface layer is uniformly heated around the periphery, the heat flow to the core is uniform in all directions.

This radial temperature difference in the billet at the end of the heating process is too important in many cases to enable the billet to be immediately extruded. Therefore, it must be equalized to a value suitable for extrusion. Naturally, the time needed depends on the material and diameter of the billet as well as on the energy input because this parameter significantly affects the developed temperature difference [7].

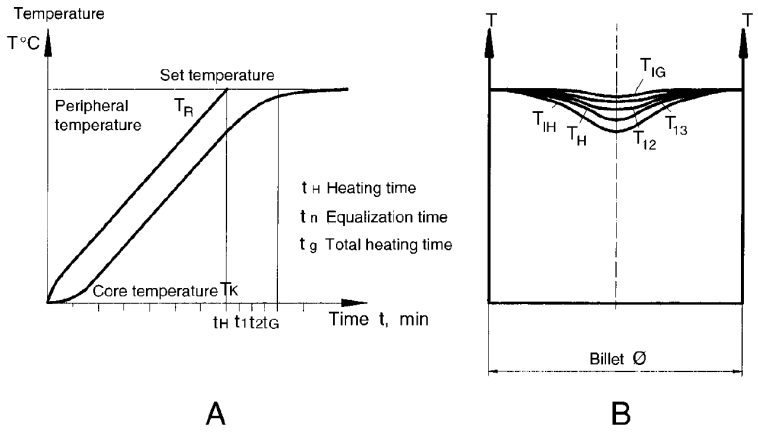


Figure 1.8 Temperature variation in heating and equalization [7]

## 1.4.2 Gas-Fired Furnace

The gas-fired furnace can be used as an alternative to induction heating for heating the billet. The fact that in many manufacturers, quite cheaper gas energy is available than electricity resulted in the expansion of these furnaces to save energy costs and produce a combustion-based furnace comparable to the induction furnace. However, in contrast to the induction furnace, where a coil is needed for each billet diameter, only one furnace tunnel, fitted to the maximum billet diameter, is used for all billet diameters [1].

Heating is done by several burners uniformly distributed on either side of the furnace tunnel over the full tunnel length Figure 1.9. To uniformly heat the billets, it is necessary to arrange the burners in several rows, one above the other, depending on the billet diameter. The exhaust gases are transferred via an exhaust duct to the entry side and then fed into a flue.

In this heating method, the entire heat input must be through the billet surface. Therefore, the energy input cannot be as high as the induction furnace. Gas-fired furnaces also require more extended time for heating than induction furnaces. A long furnace length is required for reasonable temperature control which is divided into several zones [1].

Figure 1.9 Furnace tunnel of a gas-fired furnace with nozzle boxes and nozzles for heating the billets

### 1.4.3 Rapid-Heating Gas-Fired Preheat Furnace with Billet Preheating

The difference between gas and rapid gas-Fried furnace is usage of exhaust gases which are scorching and contain considerable heat energy. And therefore, for using this very hot exhaust there is need of adequate space. A zone is added to the heated area of the gas furnace on the entry side, within which preheating is carried out with the exhaust gases [3]. These exhaust gases can be transferred by two methods, one is by using fans, and the second by with specific nozzles that are implemented in preheating zone.

The first method is, in the more straightforward but also less effective design, the gases flow in a tunnel built onto the heated zone past the billets to the entry side. Adequate turbulence of the exhaust gas flow is needed for good heat transfer.

The second preheating method uses nozzles with high velocity, which transfer the exhaust gasses to the billet's surface. However, the recycling of the exhaust gases only functions over a limited length, so the preheat section must be divided into several recycling zones or fan fields. These preheat zones have significantly higher utilization of the exhaust gas heat than the more straightforward design described previously, Figure 1.10 [1].

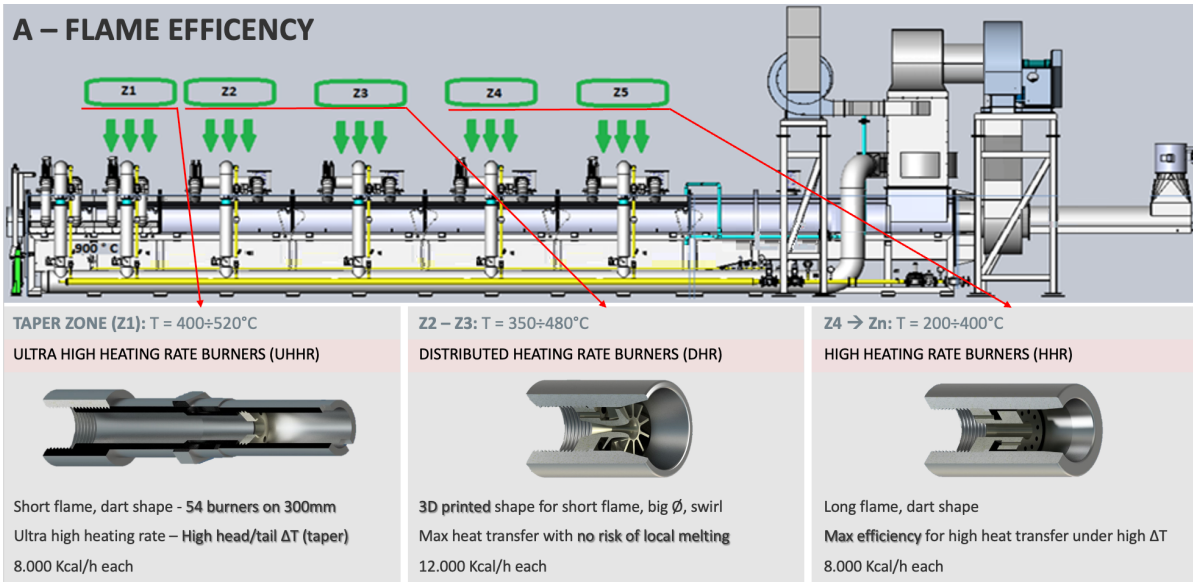


Figure 1.10 Rapid heating gas-fired furnace with nozzles with high velocity and installed fans

### 1.4.4 Combination of Induction Furnace and Rapid-Heating Gas-Fired Furnace

Despite the degree of development, the rapid-heating gas-fired furnace is not comparable to the induction furnace. Due to extended furnace size requires significantly more space and is less flexible. In addition, the induction furnace is used for reaching a higher and final temperature. This assortment is an optimization of the advantages of both furnaces. Both furnace types are used in the temperature range, which offers the best advantage. There are numerous cases where such a combination represents the best solution, always when, for example, a second furnace must be installed alongside an existing gas or induction furnace to increase throughput capacity.

The use of this combination is only reasonable and viable from an investment-cost point of view in a new installation if there will be the need for too much product, which cannot be achieved from a single furnace and a double installation is required in any case. The installation of such a combination in cases of lower throughput where one preheats furnace alone would suffice is not recommended, except with very frequent billet temperature changes [1].

## 1.4.5 Direct Resistance Heating System

Direct Resistance Heating (DRH) works with the heating of conducting materials. An electrical current (DC or AC) flows directly in the workpiece to be heated. And cause to increase the temperature due to Joule law, the electrical energy provided is transformed into heat in the material, increasing its temperature up to a value defined by thermal material capacity, convection, and radiation losses. In all applications, a DRH installation includes a contact system, cables, and transformers to directly supply the current to the workpiece to be heated [9].

Direct Resistance Heating system is in two forms of installations, one is fixed, and another one is moving workpieces. The power supply is transferred to the billet directly by using several connectors. These connectors provide the billet with constant applied voltage, and variable current during the heating process due to the variations in the temperature of material, Figure 1.11 [10].

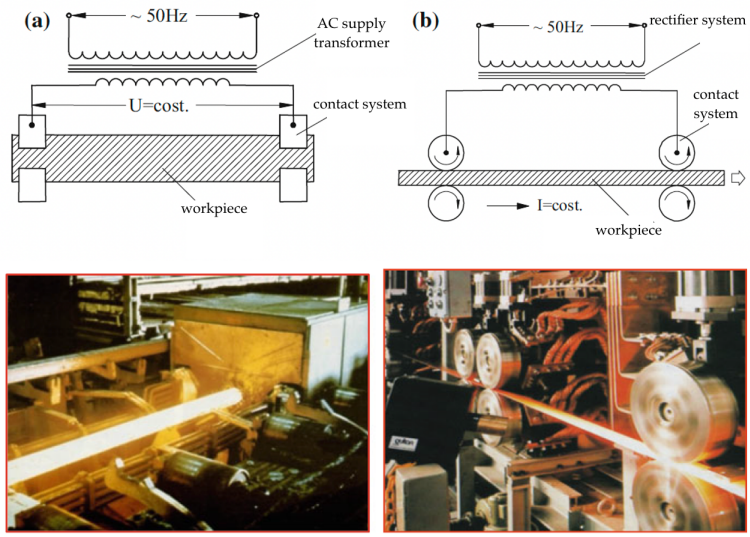


Figure 1.11 DRH installations Schematic **a** with the fixed workpiece; **b** with moving the workpiece

The contact system is responsible for injecting high currents into the load, even when the surface of the workpiece is irregular or strongly oxidized. Each contact or head typically consists of a water-cooled system to increase the contact system's efficiency.

The contact system also has high electrical and thermal conductivity, high surface hardness, and a high melting point which causes reduced resistivity to $0.4 - 0.8 \cdot 10^{-4}\ \Omega$ and losses to 1-2 kW for each head.

The number of contact system is depending on the diameter of the billet which cause the variation of injected current. There is limitation on the permissible current per point of contact that should not exceed 5–10 kA. So, for a considerable diameter value, several contacts need to handle the amount of injected current [11].

According to the workpiece diameter and high current intensity, the contact system is developed with a sufficient number of contacts, as sketched in Figure 1.12.

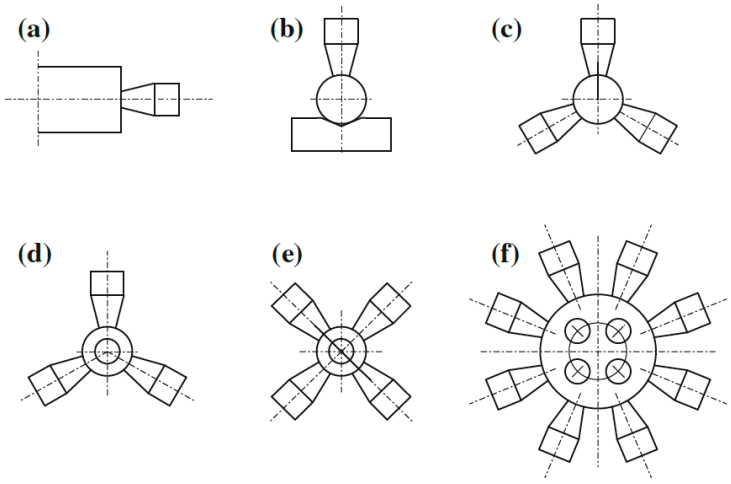


Figure 1.12 Different connection of connector

# Chapter 2

# 2 Danieli Extrusion Line

Danieli group is among the three biggest companies in the business of designing and manufacturing equipment for metal processing applications. Danieli Breda division of the group is one of the global front runners in the extrusion industry by engineering and supplying extrusion plants for processing ferrous and non-ferrous metals. The case study of this thesis work is Aluminum and Stainless-Steel processes which are extensively discussed here within.

After many years of experiments and to introduce of a highly efficient heating method, today the main methods of billet heating systems are rapid gas-fired and combination gas and induction furnace.

For what concerns Aluminum alloys, the rapid gas-fired furnace is principally used and in case of need for high-quality production processes this method can be accompanied by induction heating systems for final temperature tuning. However, when it comes to Stainless-Steel extrusion the induction heating process will be a must in order to reach higher temperatures of around 1250 ℃.

## 2.1 Rapid-Heating Gas-Fired Preheat Furnace with Billet Preheating

In Aluminium extrusion, billets initially enter in the indirect heating zone (Figure 2.2 right section) of gas furnace where the temperature of the billets is increased by very hot exhaust gasses produced in the direct heating zones (Figure 2.2 left section) of the furnace.

The Figure 2.2 is a rapid gas-fried furnace with different type of nuzzles which are implemented for each direct heating zones in order to rise the billet temperature as high as 480 ℃. The main advantage of gas heating furnaces is their fairly low CAPEX and OPEX costs.

Figure 2.1 Rapid gas-fried furnace

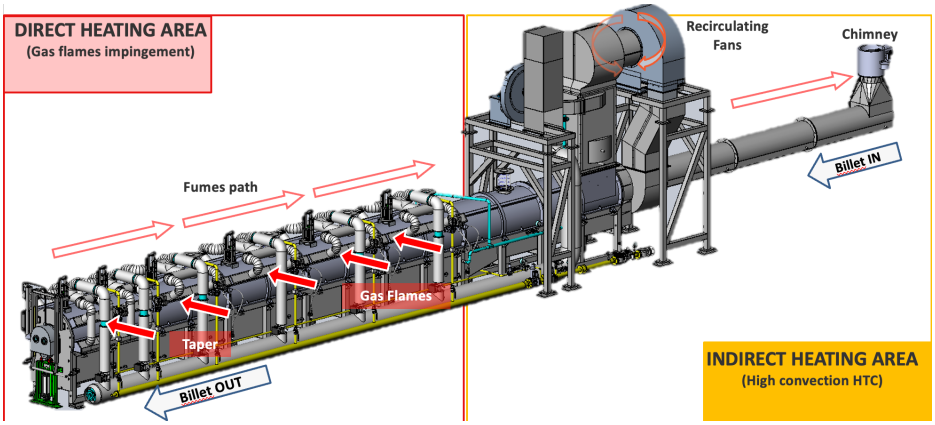


Figure 2.2 Different section of rapid-heating gas furnace

In case of Steel extrusion, instead, rotary gas furnaces are used to increase the billet temperature to much higher levels as high as 850 °C.

## 2.2 Combination of Induction Furnace and Rapid-Heating Gas-Fired Furnace

In Aluminium extrusion for increasing the efficiency of the heating process and having more precise control over the temperature ramp (over the length of the billet) the induction furnace is combined with gas furnace. In this method the billet is firstly heated by the rapid-gas furnace, and then the billet is transferred to the induction furnace for final temperature tuning.

Despite technological developments of the gas furnaces in the past years, its implementation yet has limits in terms of the precision in the heating control as also the space required for its installation. This must be also mentioned that the gas

availability is not always guaranteed in all countries and all locations. Also, in the past years the Aluminium extruded products are becoming more and more a prioritized manufacturing choice for profiles of important applications such as Automotive and Aerospace. In such applications, the consistency of the quality (mechanical properties) of the extruded profiles is a must. To guarantee a constant mechanical property over the extrusion length the billet temperature shall be controlled precisely which is obtainable by induction heating process. In such applications, the series combination of the gas heating furnaces, and the induction furnace offers a most efficient heating process in terms of overall energy cost and the temperature control.

In such combination, the Aluminium billet temperature is raised to a temperature of around 400°C (also depending on the alloy) and then is transferred to a multi-zone-controlled induction furnace where it is taper heated where the head of the billet is heated to higher temperatures with respect to its tail. This $\Delta T$ has the objective to compensate the temperature rise during extrusion process which is due heat generated from the friction between the billet and the wall of the container during extrusion.

For the Steel extrusion, instead, a rotary gas furnace (see Figure 2.3 section 1) is used to rise the temperature to much higher levels with respect to Aluminium extrusion. To further increase the temperature (more than 800 °C.) the efficiency of the rotary gas heating furnace dramatically drops in terms of heating time and the energy consumption.

This combination is shown in Figure 2.3, which is the whole schematic of the Danieli extrusion line. The billet first enters a rotary gas furnace (section 1), and after heating to a certain level, it will transfer to the induction furnace.

The induction furnace used consists of the primary (see Figure 2.3 section 2) and secondary induction furnace (see Figure 2.3 section 3) areas. The selection of each area depends on the exited temperature of a rotary gas furnace. Suppose the temperature is lower than a determined value. In that case, the billet will transfer to the primary induction to increase the temperature and then enter the second induction part to reach the final temperature. But if the temperature of the billets is high enough after the gas furnace, it is directly moved to the second induction part.

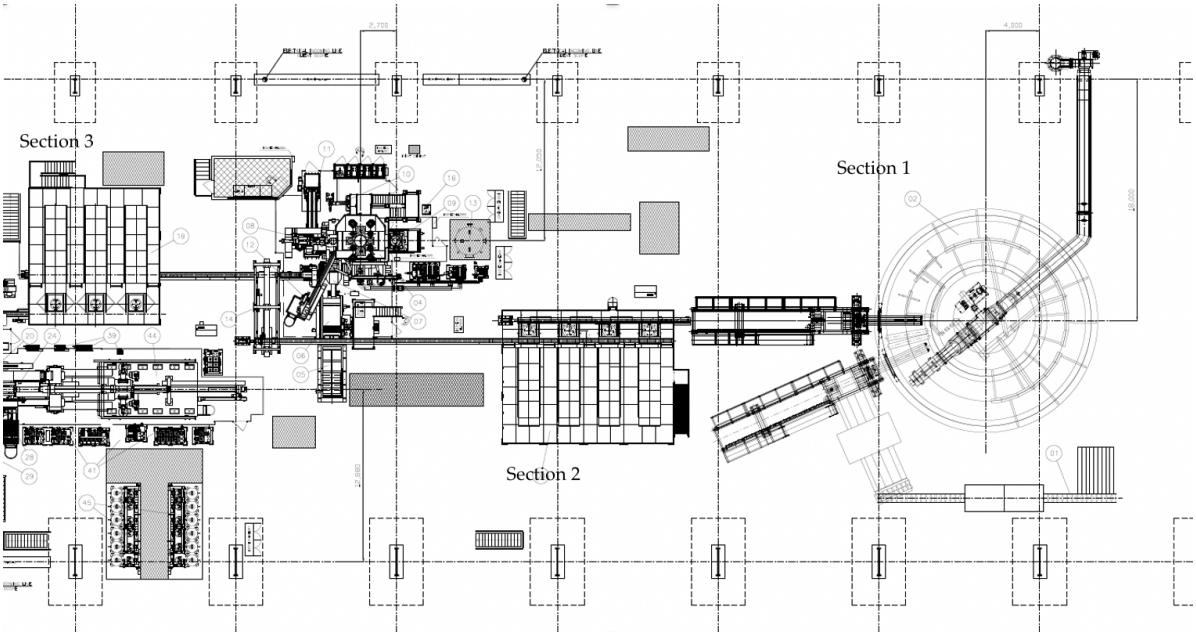


Figure 2.3 Schematic of Danieli extrusion line with rotary gas-fired furnace and with primary and secondary induction furnace

After the preheating process in the rotary gas furnace (temperature approx. 750°C), the billets will be transferred to the intermediate or in the case of the smallest diameter (i.e. ID 130mm) directly to the final heating station.

The overall heating process (gas heating and induction) is split into three phases:

**Phase 1:** preheating with a rotary gas furnace to a temperature of approx. 720 to 790 °C. In the case of the smallest diameter, the temperature in the rotary furnace will be 800 to 820 °C and the billet goes directly to the final heating station (Figure 2.3 section 3);

**Phase 2:** after heating the billet with rotary gas furnace and reaching the approximate temperature of 720 to 790 °C , the billet is transferred to the primary induction area (Figure 2.3 section 2) to increase the temperature to the value of approx. 720 to 1180 °C ;

**Phase 3:** final heating is done by secondary induction area with multizone section in induction furnace to reheat the billets and to optimize the temperature distribution by axial heating sections (Figure 2.3 section 3);

## 2.3 Data

The purpose of this study is to comparison and understand the possibility of using DRH instead of rapid gas-fried or rotary gas furnace. The gas furnace needed parameters for heating the billet can be found in Table 2.1 and Table 2.2 is obtained from studying the two main extrusion line which are Aluminum and Stainless-Steel hollow billet. The necessary parameters are related to the physical characteristics, the time and the temperature is needed for starting extrusion process.

Table 2.1 Aluminum and Stainless-Steel physical characteristic

| Subject | Unit | Aluminum solid | Stainless steel 690 Tube |
|---|---|---|---|
| **Length** | [m] | 0.6-1.3 | 0.85-1.1 |
| **Outer Diameter** | [m] | 0.2 | 0.1-0.32 |
| **Inner Diameter** | [m] | - | 0.02-0.07 |
| **ρ** | [Ωm] | $0.04 \cdot 10^{-6}$ | $0.976 \cdot 10^{-6}$ |
| **cγ** | [WS/m³ K] | $2.65 \cdot 10^{6}$ | $4.51 \cdot 10^{6}$ |
| **Thermal conductivity** | [W/mK] | 223 | 23 |

Table 2.2 Extrusion production data

| Subject | Unit | Aluminum solid | Stainless steel 690 Tube |
|---|---|---|---|
| **Initial temperature** | [°C] | 20 | 20 |
| **Final temperature** | [°C] | 450-520 | 1250 |
| **Time** | [s] | 80 | 240 |
| **Frequency** | [Hz] | 50 | 50 |

# Chapter 3

# 3 Basic Mathematics

The fact that Direct Resistance Heating generates heat directly inside the metallic body is the main reason for its success and application in several industrial applications. The heat generation inside the billet implies several positive results, notably the possibility of reaching higher production rates, higher temperature, and higher efficiency, better process control.

The main drawbacks of this kind of system are related to the geometry of the body to be heated and the maximum current that can be supplied.

Direct Resistance Heating (DRH) is based on the flow of an electrical current through the body to be heated, which is directly connected through a connector and cable to an AC or DC power supply.

When a DC current flows in the billet body of constant cross-section and constant electrical resistivity, the current density and the power density due to Joule's effect are uniformly distributed in the cross-section. Non-uniform distribution of the current density can happen if the body doesn't have a linear shape, for example, ring or bent shape, or the sizes of its cross-section change along the billet length.

In an AC current supply for the billet, the current density and inner power sources distributions will be determined by the laws of electromagnetic induction, Ohm's law, and the Joule-Lenz law [7].

Before analyzing laws and phenomena which characterize resistance heating processes, we will identify some basic ideas of the hypothesis of mathematical and electromagnetic fields.

## 3.1 Basic Mathematical

In the electro-technological procedures of conduction heating, electromagnetic phenomena are the basis for generating heat and forces inside the body to be heated. The following Section explains the fundamentals of the electromagnetic field and its impact on the current density distribution in the billet.

### 3.1.1 Maxwell Equations

Maxwell's equations are laws that are consist of a set of 4 complicated equations that express electromagnetics and straightforward ways to remark the fundamentals of electricity and magnetism.

These equations explain the electromagnetic phenomena and, in special, determine the spatial distribution of the field vectors $\overline{E}, \overline{H}, \overline{D}, \overline{B}$, including to their time dependence, as a function of the current density and the characteristics of the conductive material. These equations can be written in the form [11]:

$$\text{rot}\,\overline{H} = \bar{J} + \frac{\partial \overline{D}}{\partial t} \quad \text{(Ampere's law)}$$

$$\text{rot}\,\overline{E} = -\frac{\partial \overline{B}}{\partial t} = -\mu \cdot \frac{\partial \overline{H}}{\partial t}$$

$$\overline{D} = \varepsilon \cdot \overline{E} = \varepsilon_0 \cdot \varepsilon_r \cdot \overline{E} \qquad (3.1)$$

$$\overline{B} = \mu \cdot \overline{H} = \mu_0 \cdot \mu_r \cdot \overline{H}$$

With, $\overline{E}$ is the electric field strength; $\overline{D}$ is the electric flux density; $\overline{H}$ is the magnetic field intensity; $\overline{B}$ is the magnetic induction (flux density); $\bar{J}$ is the current density. The quantities $\varepsilon$ and $\mu$, which are respectively called electrical permittivity (or dielectric constant) and magnetic permeability, are characteristics of the material.

The parameters $\varepsilon_r, \mu_r$ denote, respectively, the relative permittivity and relative magnetic permeability. These quantities have known constant values in vacuum ($\mu_0 = 4 \cdot \pi \cdot 10^{-7}\ \text{H} \cdot \text{m}^{-1}$; $\varepsilon_0 = \frac{c^2}{\mu_0}\ \text{F.m}^{-1}$; $c = 299.792.458\ \text{km/s}$ velocity of light) [11].

### 3.1.2 Bessel Function

Bessel function is often encountered when solving boundary value problems, such as working in cylindrical coordinates. In cylindrical coordinates system, Maxwell's equation can be written as Eq (3.2).

$$\frac{d\dot{H}}{dr} + \frac{1}{r} \cdot \dot{H} = \frac{\dot{E}}{\rho}$$

$$\frac{d\dot{E}}{dr} = j \cdot \omega \cdot \mu_r \cdot \mu_0 \cdot \dot{H} \qquad (3.2)$$

Introducing new notations.

$$\xi = \frac{r}{r_e} \; ; \quad k^2 = -j \cdot \frac{\omega \cdot \mu_r \cdot \mu_0}{\rho} \cdot r_e^2 = -j \cdot m^2 \; ; \;\; m = \frac{\sqrt{2} \cdot \; r_e}{\delta} \tag{3.3}$$

From Eq (3.2) and Eq (3.3) we can reach the Eq (3.4).

$$\frac{d^2\dot{j}}{d\xi^2} + \frac{1}{\xi} \cdot \frac{d\dot{j}}{d\xi} + k^2 \cdot \dot{j} = 0 \tag{3.4}$$

The Eq (3.4) can be solved by using the Bessel function order of zero. Bessel function can be defined as a second order differential equation which is shown in Eq (3.5).

$$x^2 \cdot \frac{d^2y}{dx^2} + x \cdot \frac{dy}{dx} + (x^2 + v^2) \cdot y = 0 \tag{3.5}$$

Equation (3.5) is known as Bessel's equation. Where the solution to Bessel's equation fields Bessel functions of the first and second kind as Eq (3.6), where A and B are arbitrary constants and the constant ν, determines the order of the Bessel functions found in the solution to Bessel's differential equation and can take on any real numbered value [12].

$$y = A \cdot J_v(x) + B \cdot Y_v(x) \tag{3.6}$$

The Solution of Bessel function is Eq (3.7) and Eq (3.8).

$$\frac{d^2y}{dx^2} + \frac{1}{x} \cdot \frac{dy}{dx} - k^2 \cdot y = 0 \tag{3.7}$$

$$y = A \cdot I_0(kx) + B \cdot k_0(kx) \tag{3.8}$$

where $I_0$ and $K_0$ are Bessel functions defined as Eq (3.9) and Eq (3.10).

$$I_0(x) = 1 + \left(\frac{x}{2}\right)^2 + \frac{\left(\frac{x}{2}\right)^4}{2!^2} + \frac{\left(\frac{x}{2}\right)^6}{3!^2} + \text{etc.} \tag{3.9}$$

$$\begin{aligned} K_0(x) = I_0(x) \cdot (\ln 2 - \gamma - \ln x) + \left(\frac{x}{2}\right)^2 + \left(1 + \frac{1}{2}\right) \cdot \frac{\left(\frac{x}{2}\right)^4}{2!^2} \\ + \left(1 + \frac{1}{2} + \frac{1}{2}\right) \cdot \frac{\left(\frac{x}{2}\right)^6}{3!^2} + \text{etc.} \end{aligned} \tag{3.10}$$

Where $\gamma$ is Euler's constant 0.5772157.

If in the Eq (3.7), $K^2 = 2 \cdot j \cdot \alpha^2$ both $I_0$ and $K_0$ have $\sqrt{j}$ in their arguments. It is convenient, following Lord Kelvin, to define four new functions to separate the real and imaginary parts of the Bessel functions shown in Eq (3.11) and Eq (3.12) [13].

$$I_0\left(x\sqrt{j}\right) = \text{ber}(x) + j\,\text{bei}(x) \tag{3.11}$$

$$K_0\left(x\sqrt{j}\right) = \text{ker}\,(x) + j\,\text{kei}(x) \tag{3.12}$$

Where, ber comes from Bessel real; bei comes from Bessel imaginary; ker comes from Kelvin real; kei comes from Kelvin imaginary.

## 3.2 Phenomena Affecting the Current Density Distribution in Conductors

### 3.2.1 Skin-Effect

The skin effect is cause of an uneven distribution of the alternating electrical current in the cross-section of a conductor. The current density in the conductor due to skin effect reduce from the surface towards the internal part of the body.

When an AC current flows in the conductor (see Figure 3.1a), the current I will create a magnetic flux $\overline{B_I}$ (the direction of magnetic flux density $\overline{B_I}$ determines with the rule of the right-hand screw). This magnetic flux density $\overline{B_I}$ induces eddy current **i** in the conductor, which in turn produces a reaction magnetic field characterized by the vector $\overline{B_i}$. The induced eddy currents **i** in the conductor have the same direction on the surface of the conductor instead opposite direction in the centre of the conductor, therefore this eddy current will increase the total value of the current close to the surface, weaken it in the central part of the conductor, and cause an uneven distribution of current density in the cross-section. This phenomenon is called the Skin effect in Figure 3.1b [12].

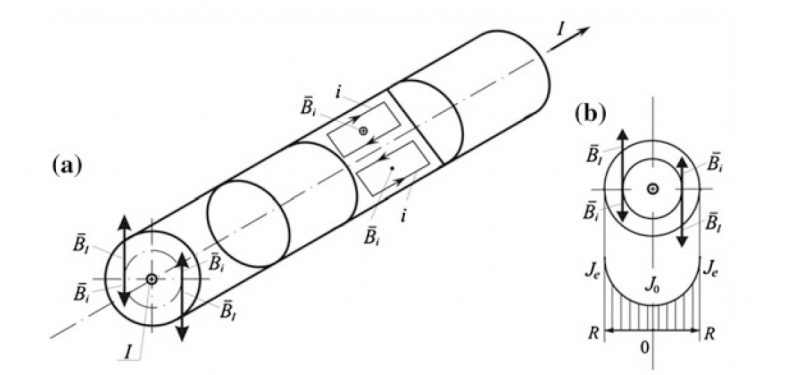


Figure 3.1 Skin-effect in a cylindrical conductor**. a** path of induced eddy current i, **b** distribution of current density J in the conductor cross-section

Due to skin effect the current density decrease from the surface towards the centre of the conductor. This current reduction can be shown by the exponential law which is shown Eq (3.14).

$$J = J_e \cdot e^{-\frac{y}{\delta}} \tag{3.14}$$

Where, J is the current density at a distance y from the surface of the conductor in $A/m^2$; $J_e$ is the current density at the conductor's surface in $A/m^2$; $\delta$ is the penetration thickness of the electromagnetic wave in m.

In a linear and homogeneous conducting material, the penetration thickness is Eq (3.15).

$$\delta = \sqrt{\frac{2 \cdot \rho}{\omega \cdot \mu_0 \cdot \mu_r}} \tag{3.15}$$

Where, $\omega = 2 \cdot \pi \cdot f$ is the pulsation of the electromagnetic field in rad/s; $\mu_r$ is the relative magnetic permeability and penetration thickness in m.

Introducing in Eq (3.15) the values $\omega = 2 \cdot \pi \cdot f$ and $\mu_0 = 4 \cdot \pi \cdot 10^{-7}$ H/m the penetration thickness can be expressed in the more convenient form in Eq (3.16).

$$\delta = \sqrt{\frac{2 \cdot \rho}{2 \cdot \pi \cdot f \cdot 4 \cdot \pi \cdot 10^{-7} \cdot \mu_r}} \tag{3.16}$$

$$\delta = 503 \cdot \sqrt{\frac{\rho}{\mu_{rf}}}$$

According to Eq (3.16) the value of the penetration thickness changes with the square root of electrical resistivity and inversely with the square root of relative magnetic permeability and frequency. Therefore, penetration thickness depends on the electromagnetic properties of the conductor's material and the applied frequency, and, at the exact frequency, it has different values in various materials.

Since the volumetric power density depends on the square of J, according with Eq (3.16), its distribution from the surface towards the interior of the conductor can be expressed by the Eq (3.17).

$$w = w_e \cdot (1 - e^{-\frac{2y}{\delta}}) \qquad (3.17)$$

With $w_e = \rho \cdot J^2$

From Eq (3.16) and Eq (3.17) we can obtain Figure 3.2, which shows the distribution of current and power density versus the distance from the surface. Figure 3.2 shows that at a penetration thickness greater than three times δ, the values of all the quantities of interest (current density, volume-specific power) are practically negligible [11].

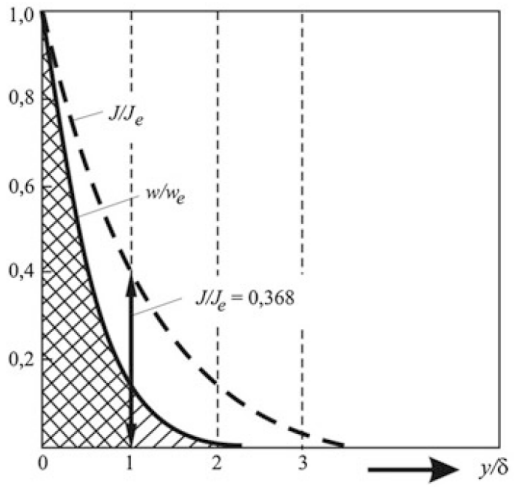


Figure 3.2 Current density (J) and power density (w) showing penetration thickness by considering the distance from the surface

It can be easily demonstrated that the ratio of the power released in the surface layer of thickness equal to the penetration thickness δ to the total active power released in the conducting semi-infinite body, is equal to:

$$P_{\delta} = P_{total} \cdot (1 - e^{-2}) = 0.865 \cdot P_{tot} \qquad (3.18)$$

The Eq (3.18) shows that the surface layer of thickness equal to the penetration depth is allocated 86.5 % of the total active power dissipated in the semi-infinite conducting body. Considering that nearly all the active power is concentrated in the surface layer of thickness δ [11].

# Chapter 4

# 4 Heat Transfer

Heat transfer occurs from a region at a higher temperature to a region with a lower temperature. And Joule is the unit to quantify energy, work, or the amount of heat Q.

## 4.1 Basics of Heat Transfer

By the consideration that there are no losses, energy entering the material by any means and will be stored as heat. During heating, the thermal gradients cause to transfer of heat from the source to the rest of the material. This moving heat is distributed non-uniformly in the volume, and it has specific heat energy (joules) in the metal at any instant. If the heat sources are switched off, and there will be an allowance time for soaking (still with no losses), this heat distributes itself in the volume until the temperature is constant throughout; this steady temperature distribution is the mean temperature rise $\theta_m$ (K). It appears in all equations as a function of time and power input since the energy input is the product of the energy input rate (J/s) and time t (s) [14].

The energy input for cylinder configuration with uniformly heated surface is given by Eq (4.1).

$$P \cdot t \cdot (2 \cdot \pi \cdot r) \cdot l \tag{4.1}$$

With, Power is in $W/m^2$, time is in s, radius and length are in m.

The energy stored is given by Eq (4.2).

$$\theta_m \cdot (\pi \cdot r^2 \cdot l) \cdot c\gamma \tag{4.2}$$

The symbol $c\gamma$ is for volume specific heat is in $J/m^3K$.

The value of $\theta_m$ is shown in Eq (4.3).

$$\theta_m = 2 \cdot P \cdot t/(R \cdot (c\gamma)) \tag{4.3}$$

The heat transfer process has three different stages first is the transient stage, the second steady temperature rise and finally switch off stage.

### 4.1.1 Transient Stage

When power is switched on and applied to the surface, the temperature rises immediately, but the heat will not transfer in the volume until the thermal gradient is established. For easier understanding of the transient stage, the material is mentally divided into layers. Before each layer can produce the temperature rise needed to transfer energy to the next layer, it must store energy in its layer proportional to the temperature rise. This creates a transient temperature rise, which is very important. The transient condition exists until every part of the material receives energy simultaneously.

### 4.1.2 Steady Temperature Rise

Steady-state temperature happens when the mean temperature increases linearly with time, whatever the actual temperature distribution in the material. When the transient is finished, and energy is flowing at the same rate into the whole volume. The temperature pattern is then fixed in shape at all instants of time.

### 4.1.3 After Switch-Off

Switching off the power, another transient condition appears. This is known as the soaking period and is needed to get approximately uniform temperatures throughout the volume before the metal is worked [15].

## 4.2 Mathematical Treatment

In the below section, all three conditions, the transient stage, steady temperature rise, and switch off stage are introduced mathematically in Eq (4.4).

$$\theta = \frac{2 \cdot P \cdot t}{R \cdot (c\gamma)} + \frac{P \cdot R}{2 \cdot \lambda} \cdot \left[ \left(\frac{r}{R}\right)^2 - \frac{1}{2} - 4 \cdot \sum_{n=1}^{\infty} \exp(-\beta_n^2 \cdot \tau) \frac{J_0\left[\beta_n \left(\frac{r}{R}\right)\right]}{\beta_n^2 \cdot J_0(\beta_n)} \right] \qquad (4.4)$$

Each of these stages is shown separately in Eq (4.4a), (4.4b) and (4.4c).

Mean temperature rise $\theta_m$ is shown in Eq (4.4a).

(4.4a)

$$\frac{2 \cdot P \cdot t}{R \cdot (c\gamma)}$$

Steady state condition Eq (4.4b).

$$\frac{P \cdot R}{2 \cdot \lambda}\left[\left(\frac{r}{R}\right)^2 - \frac{1}{2}\right] \tag{4.4b}$$

Transient stage Eq (4.4c).

$$\frac{P \cdot R}{2 \cdot \lambda}\left[4 \cdot \sum_{n=1}^{\infty} \exp(-\beta_n^2 \cdot \tau) \frac{J_0\left[\beta_n \cdot \left(\frac{r}{R}\right)\right]}{\beta_n^2 \cdot J_0(\beta_n)}\right] \tag{4.4c}$$

With, n is the number of layer that the cylinder is divided to understand in each layer how energy (θ) moves to another layer.

In equation (4.4) a new symbol τ is also introduced in the transient solution. This is defined as normalized time and is dimensionless ,Eq (4.5).

$$\tau = \frac{K \cdot t}{c\gamma} \cdot R^2 \tag{4.5}$$

Note: Up to $\tau = 0.25$ , the heat flow is in a transient state, with the surface rising faster than the centre. Suffice it to say that it becomes negligible for $\tau > 0.25$.

### 4.2.1 Generalized Values in Terms Of Surface-Centre Temperature Difference

It is helpful to have terms and curves which are general and defined in non-dimensional terms. This general form of expression can be done for Eq (4.4) by considering the temperature difference between the surface and the centre after the transient ($\tau > 0.25$) [7].

Temperature of the surface r=R is shown in Eq (4.6).

$$\theta_s = \theta_m + \frac{P \cdot R}{2 \cdot \lambda} \cdot \frac{1}{2} \tag{4.6}$$

Temperature of the center r=0 is shown in Eq (4.7).

$$\theta_c = \theta_m - \frac{P \cdot R}{2 \cdot \lambda} \cdot \frac{1}{2} \tag{4.7}$$

And, we can have Eq (4.8).

$$\theta_s - \theta_c = \frac{P \cdot R}{2 \cdot \lambda} \tag{4.8}$$

From the above equations, $\theta_s$ will always be greater than $\theta_m$ and it can be written as Eq (4.9).

$$\theta_s = \theta_m + \frac{P \cdot R}{2 \cdot \lambda} \tag{4.9}$$

## 4.3 Modes of Heat Transfer

There are three types of transferring heat, conduction, convection, radiation, Figure 4.1 [14]. In most applications, all three modes of heat transfer (conduction, radiation, and convection) happen simultaneously. The effect of increasing or decreasing each mode maybe have a different impact on a different application.

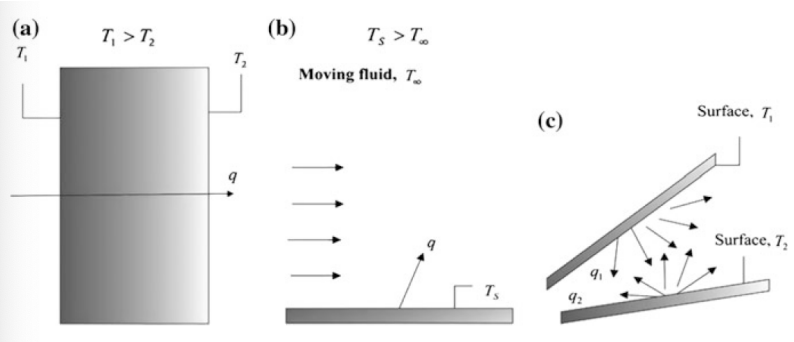


Figure 4.1 Modes of heat transfer: **a** conduction through solid or stationary fluid; **b** convection from surface to moving fluid; **c** net radiation heat exchange between two surfaces

### 4.3.1 Heat Conduction

Conduction heat transfer transfers heat through matter within solid, liquid, or gaseous or between different materials that direct physical contact is made with a different surface. Conduction is the most important heat transfer within a solid or between solid objects in thermal contact. In conduction heating, heat will transfer using the fast-

moving (in gaseous materials) or vibrating atoms (in solid materials), Figure 4.2 [14] [16].

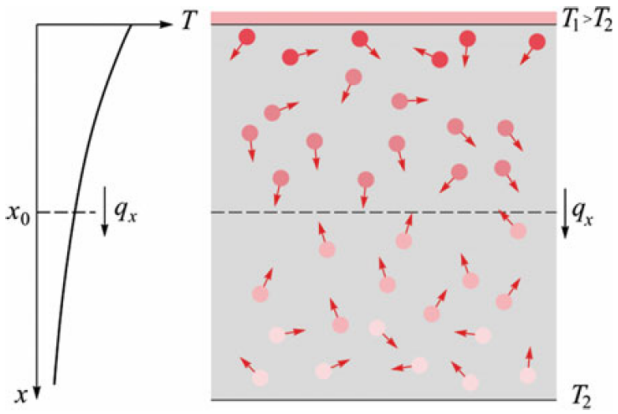


Figure 4.2 Conductive heat flux $q_x$ between heated walls at temperatures T1 and T2 due to motion of molecules.

The computation of heat conduction can be done by Eq (4.4).

### 4.3.2 Heat Convection

Convection heat is, whenever a fluid with a different temperature is in contact with a solid surface, heat transfer will occur. It also happens between two fluids or gases at different temperatures and densities. Due to our study case, I will refer only to cases in which the fluid is in contact with a solid body.

The convective heat transfer can be done in two mentioned forms.

1. natural or free convection;
2. forced or assisted convection;

In the first case, the fluid movement is produced due to viscosity differences caused by temperature variations in the fluid; the second one happens when the fluid flow is generated by motorized means, like a pump, a fan, or a mixer.

The convection heat is described by the Newton's Law which is per unit time that heat transfer through a surface. which can be expressed by the Eq (4.10).

$$q = h_c \cdot A \cdot (\theta_s - \theta_\infty) \qquad (4.10)$$

With:

| | |
|---|---|
| $q$ | heat transfer per unit time in W; |
| $A$ | area of surface in contact with the fluid in $m^2$; |
| $(\theta_s - \theta_\infty)$ | temperature difference between solid surface and the bulk fluid in °C; |
| $h_c$ | convective heat transfer coefficient in $W/(m^2°C)$; |

The temperature $\theta_\infty$ depends on the process condition. For example, $\theta_\infty$ is the temperature of the fluid outside the thermal boundary layer on a flat plate, where it is not affected anymore by the phenomenon of heat exchange, Figure 4.4.

The presence of a boundary layer near the solid surface is due to the tendency of a viscous fluid to adhere to the wall which delimits the fluid flow, thus reducing to zero the relative speed of the flow at the solid surface.

In the boundary velocity layer near the surface there are therefore strong velocity gradients, while outside it the speed tends to the undisturbed value $v_\infty$. The thickness $\delta$ of the boundary velocity layer is defined as the distance from the surface where the velocity $v$ is $v = 0.99 \cdot v_\infty$.

Figure 4.3 and Figure 4.4 illustrate the forms of the velocity and thermal boundary layers on a flat plane.

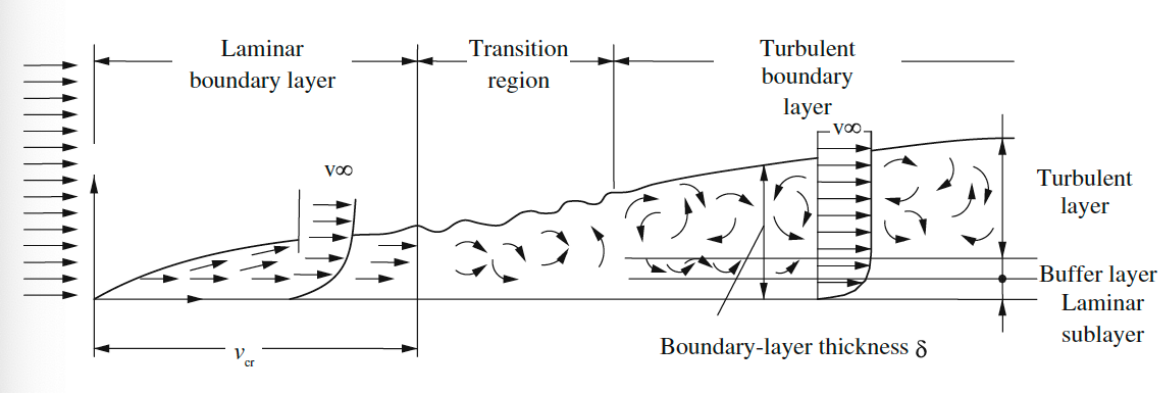


Figure 4.3 Development of the velocity boundary layer on a flat plate at different flow regimes

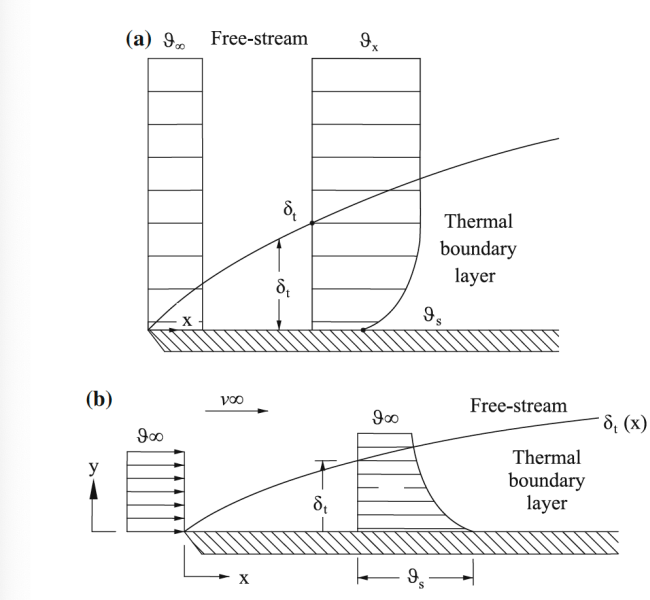


Figure 4.4 Thermal boundary layer $\delta_t$ on an isothermal flat plate: **a** $\theta_s < \theta_\infty$ ; **b** $\theta_s > \theta_\infty$ ($\theta_s$ temperature of the surface)

The thermal boundary layer thickness $\delta_t$ is defined as the distance from the surface at which the temperature difference $(\theta - \theta_s)$ equals $0.99 \cdot (\theta_\infty - \theta_s)$.

In conclusion, the convection heat transfer depends on the shape of the temperature profile in the thermal boundary layer. So, it is a complex phenomenon that is affected by several additional parameters.

- fluid properties;
- fluid stream velocity;
- fluid flow regime;
- temperatures $\theta_s$ and $\theta_\infty$ of surface and free stream;
- the geometry of the solid surface;
- surface roughness;

The determination of the heat transfer coefficient $h_c$ depends on many factors that are mentioned above, and it could be obtained only via the solution of three-dimensional, time-dependent Partial Differential Equations of Mass, Momentum, and Energy transfer governing fluid motion.

Therefore, due to this complexity for obtaining the $h_c$ a practical design value of $h_c$ is used, mostly based on the correlation of practical data. These correlations, which are valid for geometries and flow conditions, are typically expressed in terms of universal dimensionless numbers by using the following symbols [10].

| | |
|---|---|
| $d$ | diameter of cylinder in m; |
| $c_f$ | fluid specific heat in J/kg°C; |
| $\lambda_f$ | fluid thermal conductivity in W/m°C; |
| $g$ | acceleration due to gravity in $m/s^2$ ; |
| $v_m$ | mean velocity of the solid surface relative to the fluid in m/s; |
| $\Delta\theta = \theta_s - \theta_\infty$ | temperature difference between solid surface and fluid in °C; |
| $\gamma$ | density, mass per unit volume in $kg/m^3$ ; |
| $\beta_f$ | coefficient of thermal expansion of fluid in $K^{-1}$; |
| $K$ | thermal diffusivity in $m^2/s$; |
| $\mu_f$ | fluid dynamic viscosity in kg/m s; |
| $v_f$ | fluid kinematic viscosity in $m^2/s$; |
| $\varepsilon$ | emissivity of the tube surface; |

The fluid properties $\mu$, $v_f$ , $\beta_f$ and k are normally considered at the film temperature which is shown in Eq (4.11).

$$\theta_f = (\theta_s + \theta_\infty)/2 \tag{4.11}$$

The definitions and the physical meaning of the dimensionless numbers are explained in following sections.

#### 4.3.2.1 Nusselt Number

The Nusselt number is defined as the ratio of convection heat transfer to fluid conduction heat transfer under the same conditions. It is an important parameter that can contribute to a better rate of heat exchange. It is basically a function of Reynolds and Prandtl numbers [17]. It can be defined as Eq (4.12).

$$Nu = h_c \cdot d/\lambda_f \tag{4.12}$$

However, in our calculation the average Nusselt Number is used for simplicity of calculations, and it is shown in Eq (4.13).

$$\overline{Nu}_f = C \cdot (Gr \cdot Pr)_f^n \cdot \left(\frac{Pr_f}{Pr_s}\right)^{0.25} \tag{4.13}$$

with the constants C and n given in Table 5.1 as a function of $(Gr \cdot Pr)_f$.

Table 4.1 Nusselt number constant C and n as a function of $(Gr \cdot Pr)_f$

| Flow | $(\mathbf{Gr \cdot Pr})_\mathbf{f}$ | C | n |
|---|---|---|---|
| **Along vertical plane** | $10^3 \ldots . 10^9$ | 0.75 | 0.25 |
| **Along vertical plane** | $> 6 \cdot 10^{10}$ | 0.15 | 0.33 |
| **On horizontal cylinder** | $10^3 \ldots . 10^9$ | 0.5 | 0.25 |

#### 4.3.2.2 Reynolds Number

The Reynolds number Re is the ratio of inertial forces to viscous forces. The Reynolds number is a dimensionless number used to categorize the fluids systems in which the effect of viscosity is important in controlling the velocities or the flow pattern of a fluid [18]. The Reynolds number is shown in Eq (4.14).

$$\mathrm{Re} = \mathrm{v_f} \cdot \mathrm{d}/\mu_\mathrm{f} \tag{4.14}$$

#### 4.3.2.3 Prandtl Number

The Prandtl number (Pr) is a dimensionless number, named after the German physicist Ludwig Prandtl, defined as the ratio of momentum diffusivity to thermal diffusivity Eq (4.15) [19].

$$\mathrm{Pr} = \mathrm{c_f} \cdot \mu_\mathrm{f}/\lambda_\mathrm{f} \tag{4.15}$$

#### 4.3.2.4 Grashof Number

The Grashof number Gr represents the ratio of buoyancy forces due to the spatial variation of fluid density caused by temperature differences, to the restraining forces due to fluid viscosity [20].

$$\mathrm{Gr} = \mathrm{g} \cdot \mathrm{B_f} \cdot \mathrm{d}^3 \cdot \Delta\theta/\mathrm{v_f^2} \tag{4.16}$$

### 4.3.3 Radiation Losses

The radiation loss $\mathrm{P_R}$ $\mathrm{W/m^2}$ is given in Eq (4.17) by the Stefan-Boltzmann law.

$$\mathrm{P_R} = 5.67 \cdot 10^{-8} \cdot \varepsilon \cdot \mathrm{T_s^4} \tag{4.17}$$

Where, ε is the emissivity coefficient of the surface (dimensionless) and Ts is the absolute surface temperature in (K). The constant $5.67 \cdot 10^{-8}$ $W/(m^2 K^4)$ is known as Stefan's constant.

Note that the symbol for temperature has been changed here from θ to T, denoting that we are working in absolute temperatures in kelvin, If the body is radiating to a surface at absolute temperature $T_s$ kelvin, the radiation loss is reduced to:

$$P_R = \pi \cdot d \cdot 5.67 \cdot 10^{-8} \cdot \varepsilon \cdot (T_s^4 - T_a^4) \qquad (4.18)$$

$P_R$ is in W/m.

# Chapter 5

# 5 Electrical Equations

This chapter discusses the two types of Direct Resistance Heating (DRH) systems, the one with DC power supply and the other with AC power supply both at convenient frequency of 50 Hz. For what concerns the DC power supply the fundamental equations governing DC power supply are provided and discussed, then the influence of variations in material characteristics with temperature in the workpiece are studied. And, concerning AC supply of DRH, current and power density distributions in the workpiece and internal and external impedance by considering equivalent circuits have been analyzed, and governing numerical models used for our analysis are discussed.

## 5.1 DHR With DC Supply

### 5.1.1 Basic Electrical Equations

The DC power supply is used for particular geometries where the purpose of the heating process is to obtain a uniform temperature distribution in the workpiece cross-section.

#### 5.1.1.1 Simple Electrical Equations

Consider a metallic conductor, of resistivity ρ Ωm, with a uniform cross-section of area A in $m^2$ and of length $l$ in m. Then the resistance R in ohm is given by Eq (5.1).

$$R = \frac{\rho \cdot l}{A} \tag{5.1}$$

Assume that connectors are connected to the ends of the conductor and then a voltage is applied to the connectors [11]. The current I is given by Eq (5.2).

$$I = \frac{V}{R} \tag{5.2}$$

And the power dissipated in the conductor, by the Joule effect, is shown in Eq (5.3).

$$P = I^2 \cdot R = \frac{V^2}{R} \tag{5.3}$$

Equations (5.1), (5.2) and (5.3) use the circuit approach to the heating, but we shall find it useful to express those facts in their field forms. The field quantities involved are the electric field intensity E in V/m and the current density J in $A/m^2$ . From first principles, $E = \rho \cdot J$ but this can easily be obtained from Eq (5.1) and Eq (5.2).

$$I = \frac{V}{R} = \frac{V}{\rho \cdot l/A}$$

$$\frac{\rho \cdot I}{A} = \frac{V}{l} \tag{5.4}$$

$$\rho \cdot J = E$$

The field equivalent of Eq (5.3) is also can be rearranged in Eq (5.5).

$$w = I^2 \cdot R = \frac{\rho \cdot l \cdot I^2}{A} = \rho \cdot (l \cdot A) \cdot \left(\frac{I}{A}\right)^2 = \rho \cdot J^2 \tag{5.5}$$

### 5.1.1.2 Simple Electrothermal Equations

Consider a conductor with length *l*, area A, being heated with power density of w for t seconds. With no losses, energy in is equal to energy stored, and therefore we can write Eq (5.7) (see Chapter 4).

$$wt = \theta_m(c\gamma) \tag{5.6}$$

Where, $\theta_m$ is the mean temperature-rise of the material in ℃. Rearranging gives the rate-of-rise of temperature in Eq (5.7).

$$\theta_m/t = w/c\gamma \tag{5.7}$$

The basic relationships of the Ohm and Joule laws can be used in Eq (5.8).

$$I = \frac{V}{R_{dc}} = J \cdot S$$

$$P = R_{dc} \cdot I^2 = \frac{V^2}{R_{dc}} = w \cdot S \cdot l \tag{5.8}$$

| | |
|---|---|
| V, I | voltage applied to the contacts in V, and current flowing in the workpiece in A; |
| $R_{dc} = \rho \cdot L/S$ | resistance of the workpiece in Ω; |
| L,S | workpiece length in m, and area of workpiece cross-section in $m^2$; |
| J | current density in the workpiece in $A/m^2$; |
| $E = \rho \cdot J$ | electric field intensity in V/m; |
| $w = \rho \cdot J^2$ | power density in $W/m^3$; |

The energy balance of a unit volume in the workpiece is shown in Eq (5.9).

$$w \cdot \Delta t = c\gamma \cdot \Delta\theta_m \tag{5.9}$$

Using Eq (5.8) and Eq (5.9) we can reach Eq (5.10) [11].

$$w = c\gamma \cdot \frac{\Delta\theta_m}{\Delta t} \qquad P = S \cdot l \cdot c\gamma \cdot \frac{\Delta\theta_m}{\Delta t}$$

$$J = \sqrt{\frac{c\gamma}{\rho} \cdot \frac{\Delta\theta_m}{\Delta t}} \qquad I = S \cdot \sqrt{\frac{c\gamma}{\rho} \cdot \frac{\Delta\theta_m}{\Delta t}} \tag{5.10}$$

$$E = \sqrt{\rho \cdot c\gamma \cdot \frac{\Delta\theta_m}{\Delta t}} \qquad V = l \cdot \sqrt{\rho \cdot c\gamma \cdot \frac{\Delta\theta_m}{\Delta t}}$$

| | |
|---|---|
| L, S | workpiece length in m, and area of workpiece cross-section in $m^2$; |
| $c, \gamma$ | specific heat in J/kg °C, and density in $kg/m^3$; |
| $\Delta\theta_m$ | temperature increase in °C; |

## Hollow Billet Heating

In this case equations (5.10) still apply, and the specific quantities J, E and w depend on the material characteristics $(\rho, c, \gamma)$ and the temperature $\Delta\theta_m$. On the contrary, due to its smaller cross section in comparison with a solid cylindrical workpiece with the same external radius $r_e$, the integral values of current and power are considerably lower [10].

In fact, with reference to a tube of external radius $r_e$ and internal $r_i$ , using the notation $\alpha = r_i/r_e$ , if the current density is the same, the following ratios apply in Eq (5.11).

$$\frac{R_{dcbar}}{R_{dctube}} = \frac{I_{tube}}{I_{bar}} = \frac{P_{tube}}{P_{bar}} = 1 - \alpha^2 \tag{5.11}$$

As a result, for the same value of $r_e$, it is easier to achieve the values of current and power required for a certain production rate.

$$I' = \alpha \cdot I$$
$$P' = \alpha \cdot P \tag{5.12}$$

## 5.2 DRH With AC Supply

In the DRH, when introducing AC currents into workpieces of large cross-sections, a skin effect happens which generates uneven current density and volume-specific power distributions. These uneven distributions of the current and the thermal losses from the body surface will create a non-homogeneous temperature distribution over the body of the workpiece.

### 5.2.1 Distribution of Power and Current Density

It is important to understand electromagnetic phenomena when an AC current is supplied for a Direct Resistance Heating system. For analyzing the electromagnetic field, we have done some considerations: the workpiece is a long cylindrical, AC current flowing in the axial direction and sinusoidal waves. For simplicity of computation, a rough approximation is considered that is, the value of relative permeability $\mu_r$ and resistivity $\rho$ is constant during the heating period. Therefore, we can write Maxwell's equations (5.13) [12].

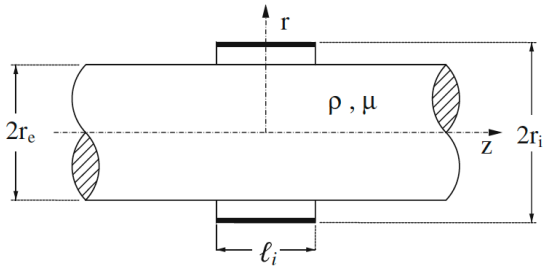


Figure 5.1 schematic of the billet

$$\text{rot}\dot{H} = \frac{\dot{E}}{\rho}\ ;\ \ \text{rot}\,\dot{\bar{E}} = -j \cdot \omega \cdot \mu \cdot \mu_0 \cdot \dot{\bar{H}} \tag{5.13}$$

In cylindrical coordinates system, $(r, \emptyset, z)$ , Maxwell's equation can be rewritten as Eq (5.14).

$$\frac{d\dot{H}}{dr} + \frac{1}{r} \cdot \dot{H} = \frac{\dot{E}}{\rho}$$
$$\frac{d\dot{E}}{dr} = j \cdot \omega \cdot \mu_r \cdot \mu_0 \cdot \dot{H} \tag{5.14}$$

From second equation (5.14) we can have Eq (5.15).

$$\frac{d\dot{H}}{dr} = \frac{1}{j \cdot \omega \cdot \mu_r \cdot \mu_0} \cdot \frac{d^2\dot{E}}{dr^2} \tag{5.15}$$

By considering that $\dot{E} = \rho\dot{j}$ and from equation (5.14) we can write.

$$\frac{d^2\dot{j}}{dr^2} + \frac{1}{r} \cdot \frac{d\dot{j}}{dr} - j\frac{\omega \cdot \mu_r \cdot \mu_0}{\rho} \cdot \dot{j} = 0 \tag{5.16}$$

Introducing dimensionless notations in Eq (5.17).

$$\xi = \frac{r}{r_e} \; ; \quad k^2 = -j \cdot \frac{\omega \cdot \mu_r \cdot \mu_0}{\rho} \cdot r_e^2 = -j \cdot m^2 \; ; \; m = \frac{\sqrt{2} \cdot r_e}{\delta} \tag{5.17}$$

And from Eq (5.17) can be written in the form

$$\frac{d^2\dot{j}}{d\xi^2} + \frac{1}{\xi} \cdot \frac{d\dot{j}}{d\xi} + k^2 \cdot \dot{j} = 0 \tag{5.18}$$

The solution of equation (5.18) can be found by definition of Bessel function (see Chapter 3) that are mentioned in Eq (5.19). With, $J_0, Y_0$ Bessel functions of order zero of first and second kind.

$$\dot{j} = \dot{C}_1 \cdot J_0(k\xi) + \dot{C}_2 \cdot Y_0(k\xi) \tag{5.19}$$

The integration constants $\dot{C}_1$ and $\dot{C}_2$ can be determined with the boundary conditions which is shown in Eq (5.20).

$$\dot{j} \neq \infty \text{ for } \xi = 0$$
$$\dot{j} = \dot{j}_e \text{ for } \xi = 1 \tag{5.20}$$

Since it is $Y_0(0) = \infty$, it must be $\dot{C}_2 = 0$, while for $\xi = 1$ it is $\dot{C}_1 = \dot{J}_e/\dot{J_0}(k)$, with $\dot{J_e}$ complex value of the current density at the surface of the cylinder.

By substitution in equation (5.19), it results is shown in Eq (5.21).

$$\dot{J} = \dot{J_e} \cdot \frac{J_0(k\xi)}{J_0(k)} = \dot{J}_e \cdot \frac{J_0(\sqrt{-j}m\xi)}{J_0(\sqrt{-j}m)} \tag{5.21}$$

Equation (5.21) is a complex value, and it is helpful to separate real and imaginary parts by using the relationship in Eq (5.22).

$$J_0\left(\sqrt{-j}x\right) = ber(x) + jbei(x) \tag{5.22}$$

Equation (5.21) can be rewrite as Eq (5.23) and Eq (5.24).

$$\dot{J} = \dot{J_e} \cdot \frac{ber(m\xi) + jbei(m\xi)}{ber(m) + jbei(m)} \tag{5.23}$$

$$\frac{|\dot{J}|}{|\dot{J_e}|} = \sqrt{\frac{ber^2(m\xi) + jbei^2(m\xi)}{ber^2(m) + jbei^2(m)}} \tag{5.24}$$

Equation (5.23) indicates that by moving from the surface towards the axis of the workpiece the current density changes. And the current density for value m > 1 has non-uniform distribution in the workpiece cross-section, while below these values, the distributions become nearly uniform as in the case of DC current, Figure 5.2 [11].

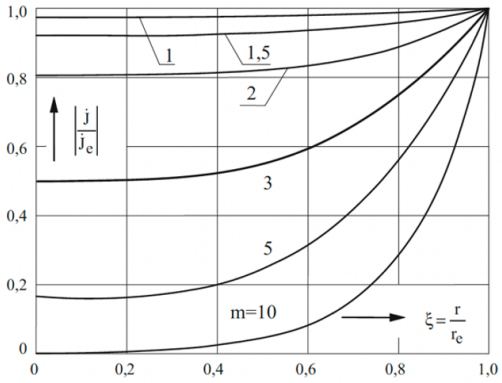


Figure 5.2 Current density distribution in a workpiece for different values of m (re, r external and generic internal radius of the workpiece; ξ = r/re; Je value of current density at surface)

The specific power per unit volume w can be reached by using the $w = \rho J^2$ and the Eq (5.24).

$$w = w_e \cdot \left(\frac{|J|}{|J_e|}\right)^2 = w_e \cdot \frac{ber^2(m\xi) + jbei^2(m\xi)}{ber^2(m) + jbei^2(m)} \qquad (5.25)$$

The Figure 5.3 is obtained from Eq (5.25) and shows that for values of $m \leq 1$ the specific power is distributed almost uniformly in the workpiece cross-section [10].

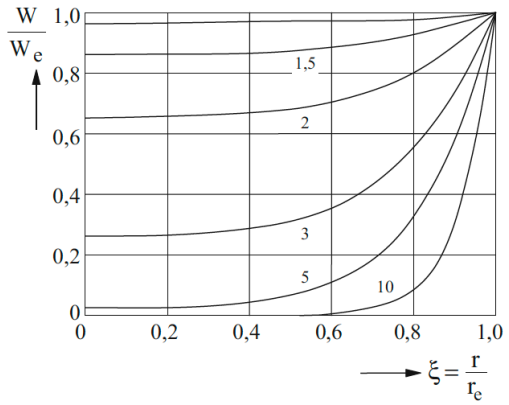


Figure 5.3 Specific power distribution in a workpiece for different values of m (re, r external and generic internal radius of the workpiece; ξ = r/re; Je value of current density at surface)

## 5.2.2 The Internal Impedance of Unit Length Workpiece

### 5.2.2.1 Solid Billet

The internal impedance unit length of the workpiece can be evaluated as Eq (5.26).

$$Z_{iu} = R_{acu} + jX_{iu} = \frac{\dot{E}_e}{I} = R_{dc1} \cdot (k_r + jk_x) \tag{5.26}$$

With, $R_{ac}$ is the AC resistance, and $X_{iu}$ is the internal reactance of the bar per unit length. $\dot{E}_e$ is the electric field intensity at the surface of the workpiece; $R_{dc1}$ is the DC resistance of unit length of the workpiece; $k_r$ and $k_x$ are the skin-effect coefficient ,Figure 5.4 [12].

$k_r$ skin effect coefficient of the internal resistance is shown in Eq (5.27).

$$K_r = \frac{R_{ac}}{R_{dc}} = \frac{m}{2} \cdot \frac{\text{ber}(m) \cdot \text{bei}'(m) - \text{bei}(m) \cdot \text{ber}'(m)}{\text{ber}^2(m) + \text{bei}^2(m)} \tag{5.27}$$

$k_x$ skin-effect coefficient of the internal reactance is shown in Eq (5.28).

$$K_x = \frac{X_i}{R_{dc}} = \frac{m}{2} \cdot \frac{\text{ber}(m) \cdot \text{bei}'(m) + \text{bei}(m) \cdot \text{ber}'(m)}{\text{ber}^2(m) + \text{bei}^2(m)} \tag{5.28}$$

The total active power in the workpiece per unit length, thus becomes in Eq (5.29).

$$P_t = R_{ac} \cdot I^2 = R_{dc} \cdot I^2 \cdot k_r \tag{5.29}$$

The diagrams of the coefficients $K_r$ and $K_x$ as a function of m are shown in Figure 5.4.

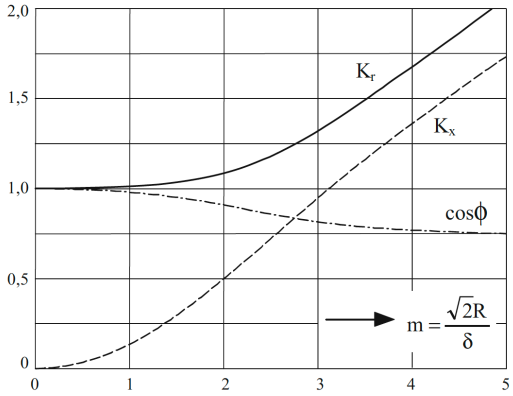


Figure 5.4 Values of skin-effect coefficients $K_r$, $K_x$ of the AC resistance $R_{acu}$ and internal reactance $X_{iu}$

An approximation can be done for low or high value m, and we can rewrite $k_r$ and $k_x$in the form of Eq (5.30), (5.31), (5,32) and (5.33) [11].

If m << 1:

$$K_r \cong 1 + \left(\frac{m^4}{192}\right) \tag{5.30}$$

$$k_x \cong \left(\frac{m^2}{8}\right) \cdot \left[1 - \frac{m^4}{384}\right] \tag{5.31}$$

If m >> 3.5:

$$K_r \cong \frac{m}{2\sqrt{2}} + \frac{1}{4} + \frac{3\sqrt{2}}{32 \cdot m} \tag{5.32}$$

$$K_x \cong \frac{m}{2\sqrt{2}} - \frac{3}{64} \cdot \left(\frac{2\sqrt{2}}{m}\right) + \frac{3}{16 \cdot m^2} \tag{5.33}$$

#### 5.2.2.2 Hollow Billet

In case of hollow billet the internal impedance of unit length of the billet is almost the same as solid billet. This change in the geometry of the billet causes changing the value of the skin-effect coefficient. And it is also shown that the coefficients $k_r$ and $k_x$ as a function of m, and it can be seen in Figure 5.5 and Figure 5.6 [12].

Note: Despite the value of m, it also must consider the ratio of the internal and external radius of billet, Eq (5.34).

$$\alpha = \frac{r_i}{r_e} \tag{5.34}$$

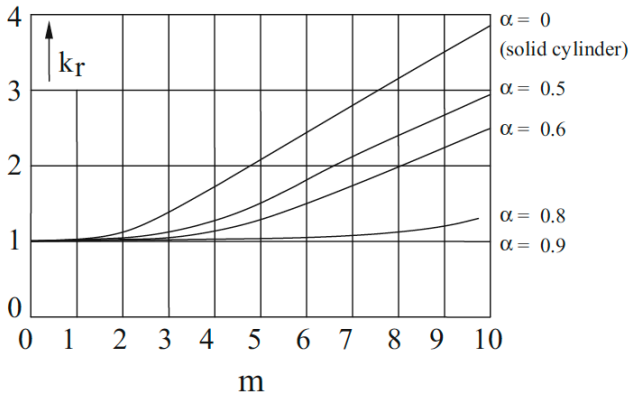


Figure 5.5 Values of skin-effect coefficients as a function of **m** for tubes of various thicknesses $K_r = R_{acu}/R_{dcu}$

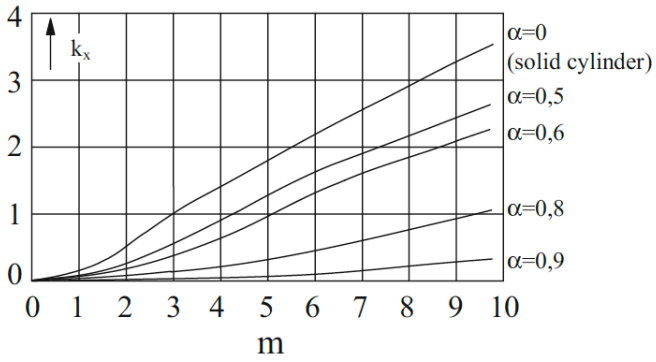


Figure 5.6 Values of skin-effect coefficients as a function of **m** for tubes of various thicknesses $K_x = X_i/R_{dcu}$

And $R_{dc}$ for hollow billet is shown in Eq (5.35).

$$R_{dc} = \rho \cdot \frac{L}{\pi \cdot r^2 \cdot (1 - \alpha^2)} \tag{5.35}$$

## 5.2.3 External Impedance

The installation of direct resistance heating devices is commonly done in the industry with a step-down transformer, a high current circuit connecting the transformer to the heating device, the contact system, and the heated workpiece. In a specific way, the external circuit of AC direct resistance heating consists of a three-phase supply transformer, adjustable phase balancing unit, control unit, single-phase transformer with primary taps and high current secondary windings, and secondary circuit comprising connecting busbars, contacts and workpiece to be heated, Figure 5.7 [11].

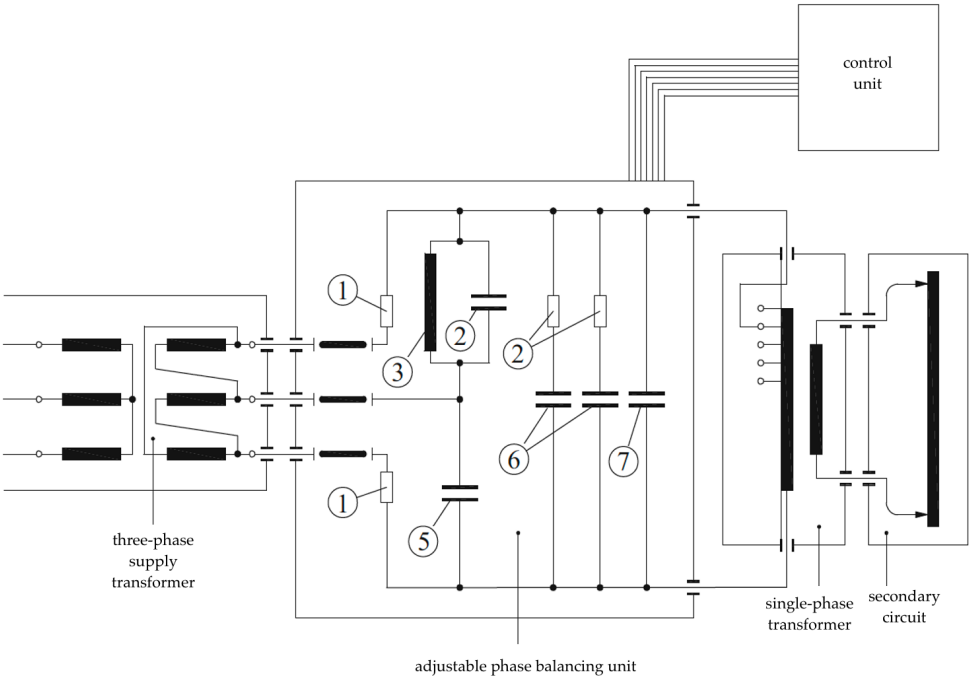


Figure 5.7 Schematic of an AC-DRH installation

## 5.2.4 Equivalent Circuit

By considering a no-load losses system of power supply transformer we can model Direct Resistance Heating installation (Figure 5.7) and get its equivalent circuits Figure 5.8a. This equivalent circuit contains resistance $R_{tr1}$ and reactance $X_{tr1}$ of the primary windings, $R_{tr2}$; $X_{tr2}$ of the secondary windings of supply transformer, $R_0$; $X_0$ its magnetizing resistance and reactance, resistance $R_{hc}$ and reactance $X_{hc}$ of the high current circuit (supply bus-bars and/or cables), resistance $R_c$ of the contact system, resistance $R_w$ and the internal reactance $X_w$ of the workpiece.

Since the no-load losses and the magnetization current of transformers used in this type of installations are quite low in comparison with their rated power and current, the magnetization branch can be neglected. And the equivalent circuit can be simplified as in Figure 5.8b, where the impedances of windings of the supply transformer are included in the resistance $R_{tr1}$ and the reactance $X_{tr1}$ [11].

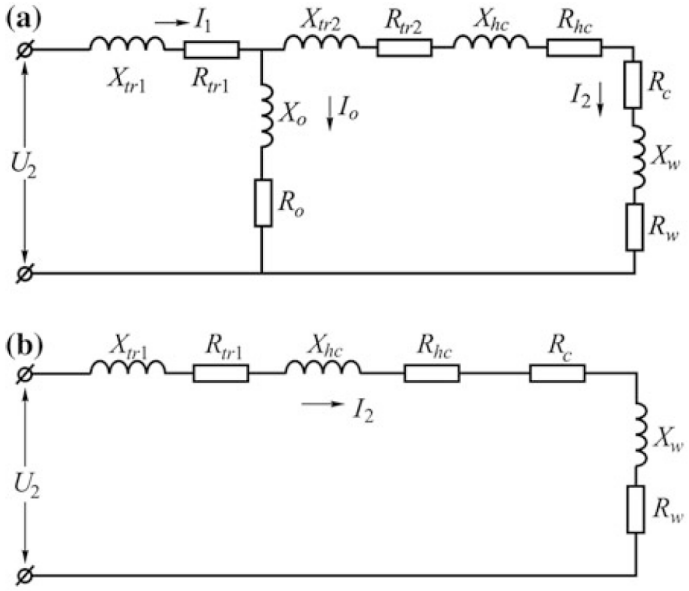


Figure 5.8 **a** Equivalent circuit of the single-phase transformer with no losses **b** neglecting the magnetization branch

The equivalent circuit of Figure 5.8 can be calculated as follow from Eq (5.36) to Eq (5.40).

The impedance of the transformer can be calculated from its plate data by the Eq (5.36). Where, u% is the percent short-circuit voltage; $U_{2n}$ is the nominal voltage on the low voltage side of the transformer in V; $I_{2n}$ nominal current on the transformer low voltage side in A.

$$Z_{tr} = \frac{U_{2n}}{I_{2n}} \cdot u\% \tag{5.36}$$

The resistance $R_{tr}$ is given by Eq (5.37).

$$P_{tr} = \frac{P_{sc}}{I_{2n}^2} \tag{5.37}$$

With, $P_{sc}$ is the short-circuit power of supply transformer in W.

The transformer reactance is shown in Eq (5.38).

$$X_{tr} = \sqrt{Z_{tr}^2 - R_{tr}^2} \tag{5.38}$$

As known, the high current circuit consists of busbars (or cables) made of Copper or Aluminium, and a contact system connecting the circuit to the workpiece. The

calculation of resistances $R_{hc}$ of the elements of this circuit must take into account skin effects. Skin effect can be considered by using the coefficients $K_r$. And for evaluation, reactance $X_{hc}$ can be evaluated by using the coefficients $k_x$. However, the values calculated in this way do not consider the mutual influence between the high current circuit elements due to the proximity effect.

The contacts which supply current to the workpiece are made usually of Copper or Bronze, And the contact resistance $R_c$ of a Copper contact system for Steel products is in the range $0.4 \div 0.8 \cdot 10^{-4}\ \Omega$.

The resistance $R_w$ and the internal reactance $X_w$ can be found in Eq (5.39).

$$\begin{aligned} R_w &= K_r \cdot R_{dc} \\ X_w &= K_x \cdot R_{dc} \end{aligned} \tag{5.39}$$

Where, $R_{dc}$ is the DC resistance of the workpiece in ohm; $K_r$ and $K_x$ are the resistance and reactance skin effect coefficients.

Total impedance of secondary circuit is shown in Eq (5.40).

$$Z = \sqrt{(R_{tr} + R_{hc} + R_c + R_w)^2 + (X_{tr} + X_{hc} + X_w)^2} \tag{5.40}$$

For understanding the general value of total impedance, the Eq (5.40) can be simplified in such a way that, the values of $R_{tr}, R_{hc}, R_c$ with respect to $R_w$ can be neglected due to higher value of $R_w$ rather than other external circuit resistance. This consideration allows us to write Eq (5.41).

$$\begin{aligned} X_e &= X_{tr1} + X_{hc} \\ Z &= \sqrt{(R_w)^2 + (X_e + X_w)^2} \end{aligned} \tag{5.41}$$

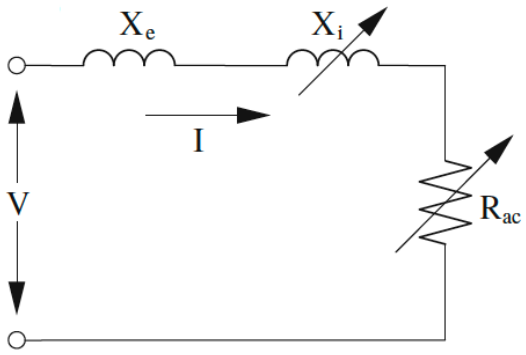


Figure 5.9 Simplified equivalent circuit of Direct Resistance Heating

For calculating the value of external reactance, instead of whole computation by equations from (5.36) to (5.39), we can use a simple and approximate way for evaluation for our study. Figure 5.10 shows the external reactance of the whole system (comprising the transformer, the high-current circuit and the connector, $X_e$) by considering the area covered by the whole system [21] [22].

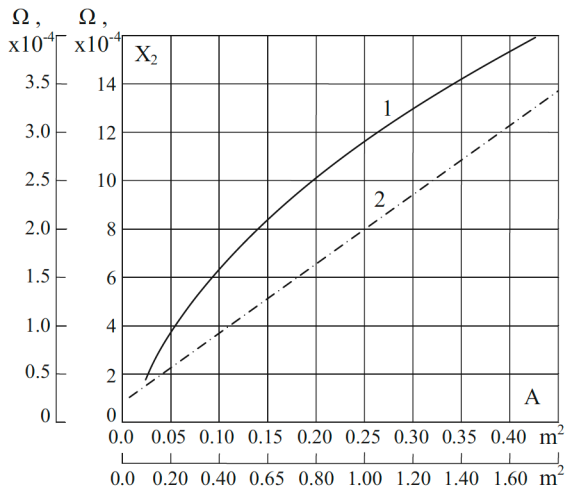


Figure 5.10 Values of reactance of a circuit as a function of its area A: (1) A < 0.4 $m^2$; (2) A = 0.1–1.6 $m^2$

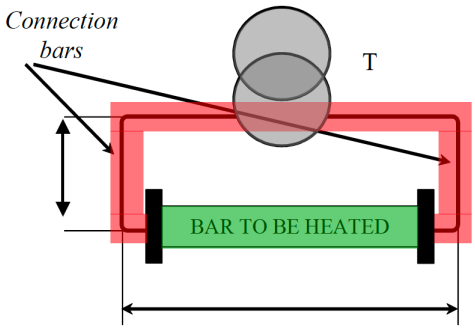


Figure 5.11 Simple schematic of Direct Resistance Heating system

# Chapter 6

# 6 Results Of Computation

To perform feasibility study of Direct Resistance Heating (DRH) application to Aluminum and Steel extrusion process, different parameters shall be taken into considerations such as power supply system type (DC or AC), electrical and thermal properties of the heated materials (Steel and Aluminum), etc. In our study we have made assumptions and approximations in order to converge to a valid result. For example, electrical and thermal losses in both DC and AC power supply DRH systems are neglected, however these assumptions shall never compromise the validity of our computations and results.

In the Table 6.1 the average physical properties (those of our interest) of Aluminum solid billet and Stainless-Steel hollow billet which are used for our study are presented.

Table 6.1 Average physical properties of Al and Steel

| Item | Unit | Aluminum solid | Stainless steel 690 Tube |
|---|---|---|---|
| **Length** | [m] | 1 | 1 |
| **Outer Diameter** | [m] | 0.1 | 0.114 |
| **Inner Diameter** | [m] | - | 0.07 |
| **ρ** | [Ωm] | $0.04 \times 10^{-6}$ | $0.976 \times 10^{-6}$ |
| **cγ** | [WS/m$^3$K] | $2.65 \times 10^{6}$ | $4.51 \times 10^{6}$ |
| **Thermal conductivity** | [W/mK] | 223 | 23 |

The Table 6.2 shows the data related to the production.

Table 6.2 Danieli production rate date

| Subject | Unit | Aluminum solid | Stainless steel 690 Tube |
|---|---|---|---|
| **Initial temperature** | [°C] | 20 | 20 |
| **Final temperature** | [°C] | 480 | 1250 |
| **Heating Time** | [s] | 50 | 240 |
| **AC Frequency** | [Hz] | 50 | 50 |

## 6.1 DRH System with DC Supply

In this section, the calculations related to temperature distribution model using DC power supply is performed using mathematical models with approximations considering that there are no thermal and electrical losses. Finally, to validate our calculations, we have used field data inputs from a Danielis' operating Gas Heating Furnace (see Tables 6.1 and Table 6.2).

As explained in Chapter 5, one important issue that must be considered is that in practice, resistivity, thermal conductivity, and specific heat of the material changes with temperature variation. To evaluate the impact of such variations, we have defined three case studies: In first case study, for the simplicity of our computations, it is considered that the characteristic of the material remains constant during the heating, and there are no thermal losses due to convection and radiation. In this case study, an average value of resistivity, thermal conductivity, and specific heat is considered during heating process. In the second case study, these constants are changing for each defined temperature interval, and an average value in each interval is considered. In this way, we can have more accurate results with respect to the first case study (see also Appendix A.4).

In two previous case studies, it is assumed that all heating process is done by DRH, increasing the temperature from 20 to 480 and 1250 ℃ respectively for Aluminum and Stainless-Steel hollow billet. However, in the third case study and only for Stainless Steel, a two-step increase is considered due to the high temperature that shall be reached for the extrusion process. Therefore, there would be a temperature increase by DRH from 20 to 700 ℃ and then transferring the billet to an induction furnace for the final heat increase.

#### 6.1.1.1 First Case Study: Constant Material Characteristics

In the first case study, the value of the physical characteristic is constant during the whole procedure meaning constant resistivity, thermal conductivity, and specific heat. This is a rough approximation, but it helps us understand the general requirements of the process in terms of necessary power and current that shall be fed into the billet. The results in the Table 6.3 are obtained by inserting the values of Table 6.1 into the equations (5.11).

Table 6.3 Direct Resistance Heating results by considering constant material during heating process for both Aluminum and Stainless-Steel tube

| subject | Unit | Stainless steel tube | Aluminum solid | Subject | Unit | Stainless steel tube | Aluminum solid |
|---|---|---|---|---|---|---|---|
| | | value | | | | value | |
| w | $w/m^3$ | $23 \cdot 10^6$ | $25 \cdot 10^6$ | P | kw | 924 | 799 |
| J | $A/m^2$ | $5 \cdot 10^6$ | $25 \cdot 10^6$ | I | kA | 194 | 791 |
| E | V/m | 5 | 1 | V | V | 5 | 1 |

### 6.1.1.2 Second Case Study: Variable Material Characteristics

The previous calculations assumed constant "average" values of material characteristics during the whole heating process. However, in reality the values of ρ , c, and γ vary with temperature. For analyzing the influence of such variations on the heating transient, the calculation must be done by updating the material characteristics with temperature. Using this consideration, the heating process is subdivided into several temperature intermissions, assuming the average value of material characteristics in each of them. Obviously, the accuracy increases as the number of intervals increases

When applying equations (5.11), it must be noted that the applied voltage across the load is constant and, consequently, the electric field intensity E remains constant. Considering variable material characteristics during the heating process, we can reach different results than the average value, especially for the high-temperature difference. In this case study, the voltage used in computation is considered constant to the voltage value which is obtained from case 1 (Table 6.3). Subsequently, for a 1-meter length billet, the value of electric field intensity E is 5 V/m for Stainless Steel tube and Aluminum 1 V or 1 V/m Table 6.4 and Table 6.6. And we can rearrange the equations (5.11) in the form of Eq (6.1).

$$\Delta t = \frac{\Delta\theta_m}{E^2} \cdot (\rho \cdot c\gamma)$$
$$J = \frac{E}{\rho} \qquad (6.1)$$
$$w = \frac{E^2}{\rho}$$

Table 6.4 Needed Data for Al

| Item | Value |
|---|---|
| **E [V/m]** | 1 |
| **r[m]** | 0.1 |
| **L [m]** | 1 |
| **S [$m^2$]** | 0.03 |

Table 6.5 Direct Resistance Heating results by considering variable material during the heating process for Aluminum

| **Temperature** | **$\rho$** $\Omega m \cdot 10^{-6}$ | **$c\gamma$** $\frac{Ws}{m^3K} \cdot 10^6$ | **$\lambda$** W/mK | **$\rho c\gamma$** | **$\Delta t$** s | **$\Sigma\Delta t$** s | **J** $\frac{A}{m^2} \cdot 10^6$ | **w** $\frac{W}{m^2} \cdot 10^6$ | **I** kA | **P** kW |
|---|---|---|---|---|---|---|---|---|---|---|
| 20 | 0.0270 | 2.52 | 211 | 0.068 | 5 | 5 | 37 | 37 | 1162 | 1162 |
| 100 | 0.0364 | 2.59 | 219 | 0.094 | 9 | 14 | 27 | 27 | 862 | 862 |
| 200 | 0.0478 | 2.65 | 224 | 0.126 | 12 | 27 | 20 | 20 | 656 | 656 |
| 300 | 0.0599 | 2.71 | 223 | 0.162 | 16 | 43 | 16 | 16 | 524 | 524 |
| 400 | 0.073 | 2.78 | 216 | 0.202 | 20 | 64 | 13 | 13 | 430 | 430 |

The result from Table 6.5 shows that the required current for heating Aluminum is too high, and it is due to the billet's low resistivity and high diameter. So, as the result, there are some restrictions such as the number of connectors and required power supply. Therefore, it is not convenient to use direct resistance heating to heat the Aluminum billets of such high diameters.

Another problem is that the voltage drops over the billet is too low and only around 1 V which is comparable with voltage drop in the external circuit and the contacts.

Table 6.6 Needed data for Stainless Steel hollow billet

| Item | Value |
|---|---|
| **E [V/m]** | 5 |
| **$r_e$[m]** | 0.11 |
| **$r_i$ [m]** | 0.07 |
| **L [m]** | 1 |
| **S [$m^2$ ]** | 0.04 |
| **α** | 0.61 |

Table 6.7 Direct Resistance Heating results by considering variable material during the heating process for Stainless Steel tube

| **Temperature** | **$\rho$** | **$c\gamma$** | **λ** | **$\rho c\gamma$** | **Δt** | **ΣΔt** | **J** | **w** | **I** | **P** | **I (tube)** | **P (tube)** |
|---|---|---|---|---|---|---|---|---|---|---|---|---|
| **Unit** | $\Omega m \cdot 10^{-6}$ | $\frac{Ws}{m^3K} \cdot 10^6$ | W/mK | | s | s | $\frac{A}{m^2} \cdot 10^6$ | $\frac{W}{m^2} \cdot 10^6$ | kA | kW | kA | kW |
| 20 | 0.695 | 4.04 | 15.9 | 2.80 | 10 | 10 | 7 | 31 | 275 | 1297 | 169 | 796 |
| 100 | 0.776 | 4.15 | 16.3 | 3.22 | 14 | 24 | 6 | 28 | 247 | 1161 | 151 | 713 |
| 200 | 0.85 | 4.24 | 17.2 | 3.6 | 16 | 41 | 5.5 | 25 | 225 | 1060 | 138 | 651 |
| 300 | 0.915 | 4.36 | 18.0 | 3.98 | 18 | 59 | 5 | 24 | 209 | 985 | 128 | 604 |
| 400 | 0.976 | 4.51 | 19.7 | 4.4 | 19 | 79 | 4.8 | 22 | 196 | 923 | 120 | 567 |
| 500 | 1.03 | 4.83 | 21.4 | 4.97 | 22 | 101 | 4.5 | 21 | 186 | 875 | 114 | 537 |
| 600 | 1.072 | 4.84 | 23.0 | 5.18 | 23 | 125 | 4.3 | 20 | 178 | 840 | 109 | 516 |
| 700 | 1.111 | 4.87 | 24.3 | 5.41 | 24 | 149 | 4.2 | 19.5 | 172 | 811 | 106 | 498 |

| | | | | | | | | | | | | |
|---|---|---|---|---|---|---|---|---|---|---|---|---|
| 800 | 1.141 | 4.9 | 26.0 | 5.5 | 25 | 174 | 4.1 | 19 | 168 | 790 | 103 | 485 |
| 900 | 1.171 | 4.86 | 27.0 | 5.69 | 25 | 200 | 4 | 18.5 | 163 | 769 | 100 | 472 |
| 1000 | 1.196 | 4.87 | 28.0 | 5.82 | 26 | 226 | 3.9 | 18.4 | 160 | 753 | 98 | 462 |
| 1100 | 1.22 | 4.93 | 29.0 | 6.01 | 27 | 254 | 3.8 | 18. | 157 | 738 | 96 | 453 |
| 1200 | 1.241 | 4.93 | 29.8 | 6.11 | 27 | 281 | 3.7 | 17.8 | 154 | 726 | 94 | 446 |
| 1300 | 1.257 | 4.93 | 30.5 | 6.19 | 28 | 930 | 3.5 | 17.5 | 152 | 717 | 93 | 440 |

Considering the results of Table 6.7, the required amount of current is also high, so it is not convenient to use the Direct Resistance Heating as mentioned in this case. Another issue for this heating method is the heating time which is too high (about 930s) in order to increase billet temperature from 20 to 1300. This means that there are great heat losses related to convection and radiation.

#### 6.1.1.3 Third Case Study: Increasing temperature step by step

In the typical steel extrusion process, the heating process is divided in two steps; first is the use of rapid gas furnace to works with a rapid gas furnace and the second part induction heating devices. The rapid gas furnace is used to increase the temperature of the billets to a specific value, which in our case is 700 ℃, and then transfer the billet to the induction unit.

Table 6.8 Direct Resistance Heating results by considering variable material during the heating process for Stainless Steel hollow billet with increasing temperature step by step

| **Temperature** | **$\rho$** | **$c\gamma$** | **$\lambda$** | **$\rho c\gamma$** | **$\Delta t$** | **$\Sigma\Delta t$** | **J** | **w** | **I** | **P** | **I (tube)** | **P (tube)** |
|---|---|---|---|---|---|---|---|---|---|---|---|---|
| **Unit** | $\Omega m \cdot 10^{-6}$ | $\frac{Ws}{m^3K} \cdot 10^6$ | W/mK | | s | s | $\frac{A}{m^2} \cdot 10^6$ | $W/m^2 \cdot 10^6$ | kA | kW | kA | kW |
| 20 | 0.695 | 4.04 | 15.9 | 2.80 | 10 | 10 | 6.5 | 31 | 275 | 1297 | 169 | 796 |
| 100 | 0.776 | 4.15 | 16.3 | 3.22 | 14 | 24 | 6 | 28 | 247 | 1161 | 151 | 713 |
| 200 | 0.85 | 4.24 | 17.2 | 3.6 | 16 | 41 | 5.5 | 25 | 225 | 1060 | 138 | 651 |

| | | | | | | | | | | | | |
|---|---|---|---|---|---|---|---|---|---|---|---|---|
| 300 | 0.915 | 4.36 | 18.0 | 3.98 | 18 | 59 | 5. | 24 | 209 | 985 | 128 | 604 |
| 400 | 0.976 | 4.51 | 19.7 | 4.4 | 19 | 79 | 4.8 | 22 | 196 | 923 | 120 | 567 |
| 500 | 1.03 | 4.83 | 21.4 | 4.97 | 22 | 101 | 4.5 | 21 | 186 | 875 | 114 | 537 |
| 600 | 1.072 | 4.84 | 23.0 | 5.18 | 23 | 125 | 4 | 20 | 178 | 840 | 109 | 516 |
| 700 | 1.111 | 4.87 | 24.3 | 5.41 | 24 | 149 | 4 | 19 | 172 | 811 | 106 | 498 |

The results from Table 6.8 shows that, even by reducing the heating time to 149 s from 240 s, feeding a high current into the workpiece is still needed. So, the physical issues related to connectors and external circuits still exist.

### 6.1.2 Thermal Solution

In the following, the assumption of no losses is no more considered, and the thermal problems related to convection and radiation losses of the heating the billet are introduced for the case study number two and three.

#### 6.1.2.1 Second Case Study: Variable Material Characteristic

In this case study only, Stainless Steel is considered in our analysis. For calculating the heat losses, first it is needed to find the value of the fluid properties μ, $v_f$ , $\beta_f$ and $\lambda$ and it can be done by computing the film temperature Eq (4.11) and using Table 6.2.

$$\theta_f = (\theta_s + \theta_a)/2$$

$$\theta_f = \frac{1300 + 20}{2} = 660 \cong 700$$

The value of fluid dynamic viscosity $\mu_f$ ,fluid kinematic viscosity $v_f$ , coefficient of thermal expansion of fluid $\beta_f$ and thermal conductivity λ by considering the film temperature can be found in the Table A.1 and Table A.2 of Appendix A. And, the emissivity of the tube Stainless Steel type surface, 301, can be found in Table A.3 Appendix A.

The needed data for calculating both radiation and convection losses written in the Table 6.9.

Table 6.9 The value of the dry air properties $\mu_f$ ,$v_f$ , $\beta_f$ and $\lambda_f$ at film temperature 700°C

| Item | Unit | Value |
|---|---|---|
| **d** | [m] | 0.22 |
| **ε** | - | 0.57 |
| **$\theta_s$** | [°C] | 1300 |
| **$\theta_a$** | [°C] | 20 |
| **$T_s$** | [K] | 1573 |
| **$T_a$** | [K] | 293 |
| **$\beta_f$** | $[K^{-1}]$ | $1.03 \cdot 10^{-3}$ |
| **$v_f$** | $[m^2/s]$ | $98.1 \cdot 10^{-6}$ |
| **$\lambda_f$** | [W/mK] | $5.8 \cdot 10^{-2}$ |
| **$P_{rf}$** | - | 0.703 |
| **$P_{rs}$** | - | 0.72 |

Note: the value of Prandtl numbers at film $P_{rf}$ and surface $P_{rs}$ temperature is written in Appendix Table A.1.

The radiation losses can be computed by using Eq (4.18) we can get the radiated power to ambient unit per length $P_{ur}$ and that is.

$$P_{ur} = \pi \cdot d.\, 5.67 \cdot 10^{-8} \varepsilon \cdot (T_s^4 - T_a^4)$$

$$P_{ur} = 136.7 \cong 137 \frac{kw}{m}$$

The convection losses can be computed by calculating dimensionless numbers (see Chapter 4).

The value of Nusselt number Eq (4.13) at the film temperature.

$$\bar{N}u_f = 0.5 \cdot (Gr \cdot Pr)_f^{0.25} \cdot \left(\frac{Pr_f}{Pr_s}\right)^{0.25}$$

Grashof number at film temperature (Eq (4.16)).

$$Gr_f \cdot Pr_f = \frac{g \cdot \beta \cdot d^3 \cdot \Delta\theta}{V_a^2} \cdot Pr_f$$

$$= \frac{9.8 \cdot 1.03 \cdot 10^{-3} \cdot 0.22^3 \cdot 1280}{(98.1 \cdot 10^{-6})^2} \cdot 0.703$$

$$= 1.004 \cdot 10^7$$

The Nusselt number value is.

$$\bar{N}u_f = 0.5 \cdot (1.004 \cdot 10^7)^{0.25} \cdot \left(\frac{0.703}{0.72}\right)^{0.25}$$

$$Nu = 28$$

There for the heat transfer coefficient is (Eq (4.12)).

$$h_c = Nu \cdot \frac{\lambda_f}{d}$$

$$= 28 \cdot \frac{5.8 \cdot 10^{-2}}{0.22}$$

$$= 7.4 \ \frac{w}{m^2 K}$$

Finally, convection losses are:

$$P_{uc} = h_c \cdot \pi \cdot d \cdot (\theta_s - \theta_a)$$

$$= 7.4 \cdot \pi \cdot 0.22 \cdot (1300 - 20)$$

$$= 6.5 \cong 7 \ \frac{kw}{m}$$

And total losses (radiation and convection heat losses).

$$P_{u_{total}} = P_{ur} + P_{uc}$$

$$= 137 + 7$$
$$= 144 \ \frac{kw}{m}$$

#### 6.1.2.2 Third Case Study: Increasing Temperature Step by Step

By changing the final temperature to 700 ℃ there is need of recomputing the film temperature at 700 ℃. And the value of the dry air properties $\mu_f$ ,$v_f$ , $\beta_f$ and $\lambda_f$ at film temperature can be get from Appendix Table A.1, A.2 and A.3.

The value of the film temperature is:

$$\theta_f = \frac{700 + 20}{2} = 360 \cong 400$$

The value of the dry air properties $\mu_f$ ,$v_f$ , $\beta_f$ and $\lambda_f$ at film temperature is shown in Table 6.10.

Table 6.10 The value of the dry air properties $\mu_f$ ,$\nu_f$ , $\beta_f$ and $\lambda_f$ at film temperature 400 ℃

| Item | Unit | Value |
|---|---|---|
| **d** | [m] | 0.22 |
| **ε** | - | 0.57 |
| $\boldsymbol{\theta_s}$ | [℃] | 700 |
| $\boldsymbol{\theta_a}$ | [℃] | 20 |
| $\mathbf{T_s}$ | [K] | 973 |
| $\mathbf{T_a}$ | [K] | 293 |
| $\boldsymbol{\beta_f}$ | $[K^{-1}]$ | $1.52 \cdot 10^{-3}$ |
| $\boldsymbol{\nu_f}$ | $[m^2/s]$ | $57.5 \cdot 10^{-6}$ |
| $\boldsymbol{\lambda_f}$ | [W/mK] | $4.5 \cdot 10^{-2}$ |
| $\mathbf{P_{rf}}$ | - | 0.676 |
| $\mathbf{P_{rs}}$ | - | 0.7 |

Radiation Heat Losses.

$$P_{ur} = 20 \ \frac{kW}{m}$$

Convection Heat Losses.

$$G_{ra} \cdot P_{ra} = 3.2 \cdot 10^7$$

$$Nu = 37$$

$$h_c = 7.5 \ \frac{W}{m^2 K}$$

$$P_{uc} = 3.5 \ \frac{kW}{m}$$

Total losses (convection and radiation losses).

$$P_{utotal} = 23.5 \cong 24 \ \frac{kW}{m}$$

## 6.2 DRH With AC Supply

In the Direct Resistance Heating, the calculation results of the system are strongly influenced by the variations of material characteristics during heating. Moreover, during the heating of the workpiece, when temperature increases, usually the electrical resistivity increases, giving rise to non-uniform distributions of the current density. This variation of material causes that, when AC current flows in the workpiece, uneven distributions of power and current density will occur for values of m greater than one (see Figure 5.2 and Figure 5.3 in Chapter 5).

In our study in this section, we have considered the flow of an alternating current in a metallic homogeneous cylindrical workpiece with the following assumptions; neglecting the end effect due to the uneven current density distribution near the contact system, constant material characteristic of the workpiece, and the number of connectors is two.

By considering the result of Direct Resistance Heating with DC power supply as we understood, due to good conductivity of Aluminum, it is not convenient to heat the Aluminum billet with such method and as per results obtained in our third case study the best way to increase the temperature is in step by step manner. Therefore, in the following paragraph, we just consider the Stainless-Steel hollow billet by using the two-step heating process which is increasing the temperature up to a certain point of 700 ℃.

Note: The data required for computation can be found in Tables 6.1 and Table 6.2.

Average required heating power (neglecting losses) in the temperature range 20 to 700 ℃.

$$P = \pi \cdot r_e^2 \cdot lc\gamma \cdot \frac{\Delta\theta_m}{\Delta t}$$
$$= \pi \cdot 0.1^2 \cdot 1 \cdot 4.51 \cdot 10^6 \cdot \frac{680}{240}$$
$$= 400\ \text{kW}$$
$$\text{or}$$
$$= 636\ \text{kW/m}^2$$

$\alpha$ coefficient (ratio between internal and external radius see Eq (5.34) in Chapter 5).

$$\alpha = \frac{r_i}{r_e}$$
$$= \frac{0.07}{0.1}$$

$$= 0.7$$

DC resistance of the hollow billet at beginning of heating (see Eq (5.35) in Chapter 5).

$$R_{dc} = \rho \cdot \frac{l}{\pi \cdot r_e^2 \cdot (1 - \alpha^2)}$$

$$= 0.976 \times 10^{-6} \cdot \frac{1}{\pi \cdot 0.1^2 \cdot (1 - 0.7^2)}$$

$$= 6 \cdot 10^{-3}\ m\Omega$$

To know the required value of external reactance of supply circuit (the transformer, the high-current circuit, and the connector), it is necessary to understand the characteristics of the external circuit, for example, the diameter of the cable and their positions with respect to each other, number and positions of contacts that are used to transfer the current to the workpiece and other necessary elements and their physical characteristics.

The Figure 6.1 shows the DRH in a simple way that consists of transformers, cables and contact systems. The value of external reactance can be found by Figure 5.10 that illustrate the area covered by the high current circuit. For calculating the area covered by the external circuit, we assumed that the billet length is around 1 meter, supposing that the whole system is compact. It can be assumed the entire area covered by this compact system is 2 $m^2$, so it can be seen from Figure 5.10 that the value of $X_e$ is around $4 \times 10^{-4}$ Ω.

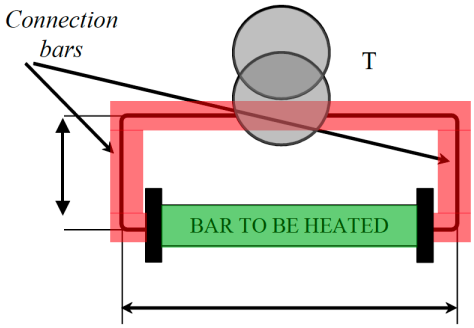


Figure 6.1 Simple schematic of Direct Resistance Heating system

Penetration thickness can be found by Eq (3.16).

$$\delta = 503 \cdot \sqrt{\frac{\rho}{\mu f}}$$

$$= 503 \cdot \sqrt{\frac{0.976 \cdot 10^{-6}}{50}}$$

$$= 7 \cdot 10^{-2}\ m$$

Value of m can be found by Eq (5.17).

$$m = \frac{\sqrt{2} \cdot r_e}{\delta}$$

$$= \frac{\sqrt{2} \cdot 0.1}{7 \cdot 10^{-2}}$$

$$= 2$$

Skin-effect coefficients $k_r$, $k_x$ can be obtain form Figure 6.5 for value of m=2 and $\alpha = 0.7$ .

$$K_r = 1$$

$$K_x = 0.1$$

AC resistance and internal reactance of the workpiece can be found by using Eq (5.39).

$$R_w = K_r \cdot R_{dc}$$

$$= 6 \cdot 10^{-3}\ m\Omega$$

$$X_w = K_x \cdot R_{dc}$$

$$= 0.6 \cdot 10^{-3}\ \ m\Omega$$

Total current:

$$I = \sqrt{\frac{P}{R_w}}$$

$$= \sqrt{\frac{400 \cdot 10^3}{6 \cdot 10^{-6}}}$$

$$= 260\ KA$$

Equivalent impedance of the system (see Chapter 5 Eq (5.40)).

$$Z = \sqrt{(R_{tr} + R_{hc} + R_c + R_w)^2 + (X_{tr} + X_{hc} + X_w)^2}$$

Due to higher value of billet resistance $R_w$ rather than external circuit resistance it is useful to do an approximation on Eq (5.40) and it can be rewrite as Eq (5.41).

$$Z_e = \sqrt{R_w^2 + (X_w + X_e)^2}$$

$$= \sqrt{(6 \cdot 10^{-6})^2 + (0.6 \cdot 10^{-6} + 0.4 \cdot 10^{-3})^2}$$

$$= 0.4\ m\Omega$$

Note 2: $X_e = X_{tr} + X_{hc}$

Supply voltage:

$$V = Z_e \cdot I$$

$$= 104\ V$$

### 6.2.1 Thermal Solution

Assuming no losses in Direct Resistance Heating with AC supply, due to skin effect the surface temperature is much higher than the center at the beginning of heating process. Therefore, a soaking time is required to allow the heat transfer from the surface to the center of the billet. Therefore, it is essential to understand how much power and time is needed to avoid exceeding the melting point of the surface by considering the required production throughput of the extrusion line that shall be satisfied.

The surface temperature of the billet is computed by using the data from Tables 6.1 and Table 6.2 and using Eq (4.6). With $\theta_m = 700\ ℃$ and $P = 634\ kW/m^2$ from above computation.

$$\theta_s = \theta_m + \frac{Pr}{4\lambda}$$

$$= 700 + \frac{634 \cdot 10^3 \cdot 0.1}{4 \cdot 23}$$

$$= 1390\ ℃$$

The above calculation for the surface temperature is valid when normalised time $\tau$, which is dimensionlessthe, is higher than 0.25. And it can be written as below:

$$\tau = \frac{\lambda \cdot t}{c\gamma \cdot r^2}$$

$$= \frac{23 \cdot 240}{4.51 \cdot 10^6} \cdot 0.1^2$$

$$=0.06$$

Since the value of $\tau = 0.06$ and it is less than 0.25, the transient heating is still present, and the surface temperature is even greater than calculated.

# Chapter 7

# 7 Conclusions and Future Works

This research aimed to verify the possibility of replacing Rapid Gas-Fried heating furnaces with Direct Resistance Heating furnace in the Aluminium and Steel Extrusion plants.

Our study clearly showed the limitations and problems related to using a DRH system (instead of a typical gas furnace) which are related to electrical, thermal, production throughput and economic issues.

The first and the most critical issue is related to the electrical limitations, making using DHR impossible for this kind of application due to the billet diameter which is both high and variable. In specific, due to high diameter of the billet the amount of required current is too high.

Besides the high value of required current to be fed into the workpiece, the subtle voltage drop on some applications is also an issue; for example, in case of Aluminium alloy billets, the voltage drop across the billet is too low, which is comparable with voltage drop on an external circuit.

The next important limitations are related to thermal problems. In the case of the DC power supply, we have uniform temperature distribution. But, in the case of AC supply, due to the skin effect, the surface temperature is much higher than the centre. This creates two main issues: one is a need for a soaking time so that temperature distribution will be uniform all over the billet. Another is to avoid reaching the melting temperature at billet surface. The other issue is related to heat losses to the ambient due to convection and radiation, so there is a need of designing an isolated system.

Another limitation is that, from the process point of view, the size of the billet varies depending on the material and the profile which is needed. These variations in the case of a gas furnace are not having much influence on the heating process because the design of the gas furnace can adopt such variations. But in DRH system, such variations in diameter significantly impact the power injected into the billet, number and position of connectors, and the design of the external circuit.

Finally, from an economic point of view, the cost of electricity is higher than gas; the system is complex compared to the gas furnace, so design cost is higher. Furthermore,

due to direct contacts of connectors with high temperature billet, there is a need of frequent maintenance.

Therefore, due to all above-mentioned limitations and obstacles, it is not convenient to use Direct Resistance Heating system in the extrusion process for billet with diameter higher than a certain value.

# 8 References


[1] M. B. G. S. K. Siegert, Extrusion, ASM International; 2nd edition, (December 1, 2006).

[2] S.-S. S. R.-S. K. S. V. Kalpakjian, "Manufacturing Engineering and Technology," *Pearson Education South Asia Pte Ltd,* 2014.

[3] D. Y. J. Rahul R, "A study on metal extrusion process," *Advanced Materials Research,* 2018.

[4] M. P. D. E. 5-Lucia O, "Induction heating technology and its applications: past developments, current technology, and future challenges.," *IEEE T Ind Electron ,* 2014.

[5] F. V. a. B. K. 6-Smolyanov I, "Research of the induction heating installation on based autoclave," in *18th international conference on computational problems of electrical engineering (CPEE)*, New York, 2017.

[6] Z. S. 7-Semiatin, Elements of induction heating: design, control, and applications, Cleveland, OH: ASM International, 1988.

[7] E. J. 9-Davies, Conduction and Induction Heating, 1990.

[8] Y. Y. M. T. 8-Oki Y, "Analysis of temperature distribution in a billet by induction heating," *Journal of Japan Institute of Light Metals,* 1990.

[9] F. Roberto, Distribuzione e applicazioni dell'energia elettrica.

[10] S. 10- Lupi, Fundamentals of Electroheat, 2017.

[11] S. 11-Lupi, Fundamentals of electroheat: Electrical technologies for process heating, 2016.

[12] B. G. Korenev, Bessel Functions and Their Applications, 2002.

[13] F. Bowman, Introduction to Bessel Functions, 1939.

[14] W. T. Von Böckh P, Heat transfer: Basics and practice, 2012.

[15] Han J, Analytical Heat Transfer, 2016.

[16] M. K. W. Majid G, Fundamental of heat transfer, 2020.

[17] E. Nagy, Basic Equations of Mass Transport Through a Membrane Layer, 2019.

[18] J. S. Bill Rehm, Managed Pressure Drilling, 2008.

[19] H. S. R. B. A. R. Chen, Encyclopedia of Agricultural, Food, and Biological Engineering, 2010.

[20] F. M. A. 12-Lupi S, Induction and direct resistance heating: Theory and numerical modeling, 2015.

[21] D. Romanov, Direct Resistance Heating of Metals, 1981.

[22] S. F. M. Lupi, "Characteristics of installations for direct resistance heating of ferromagnatic bars of square cross-section.," in *Proceedings of International Science Collection "Modelling for Electromagnetic Processing",*, Hannover (Germany), 2008.

[23] S. L. –. M. F. -. A. Aliferov, "Characteristics of Installations for Direct Resistance Heating ofFerromagnetic Bars of Square Cross-section," in *nternational Scientific Colloquium*, Hannover, October 27-29, 2008.

# 9 Appendix

## 9.1 Appendix Table A.1: Characteristics of Dry Air at Atmospheric Pressure

| $\vartheta$ | $\gamma$ | $c \cdot 10^{-3}$ | $\lambda \cdot 10^{2}$ | $a \cdot 10^{6}$ | $\mu \cdot 10^{6}$ | $\nu \cdot 10^{6}$ | Pr |
|---|---|---|---|---|---|---|---|
| °C | $Kg/m^3$ | kJ/(kg K) | W/(m K) | $m^2/s$ | Pa s | $m^2/s$ | |
| Temperature | Mass density | Specific heat content at constant pressure | Thermal conductivity | Coefficient of thermal diffusivity | Coefficient of dynamic viscosity | Coefficient of cinematic viscosity | Prandtl number |
| −50 | 1.534 | 1.013 | 2.034 | 13.15 | 1.460 | 9.54 | 0.728 |
| −20 | 1.365 | 1.010 | 2.283 | 14.02 | 1.627 | 11.93 | 0.716 |
| 0 | 1.252 | 1.010 | 2.371 | 18.77 | 1.725 | 13.70 | 0.707 |
| 20 | 1.164 | 1.013 | 2.521 | 21.30 | 1.822 | 15.70 | 0.703 |
| 40 | 1.092 | 1.013 | 2.650 | 24.02 | 1.920 | 17.60 | 0.699 |
| 60 | 1.025 | 1.018 | 2.800 | 26.83 | 2.010 | 19.60 | 0.696 |
| 80 | 0.968 | 1.021 | 2.930 | 29.60 | 2.097 | 21.70 | 0.692 |
| 100 | 0.916 | 1.021 | 3.070 | 32.80 | 2.176 | 23.78 | 0.688 |
| 140 | 0.827 | 1.026 | 3.324 | 39.20 | 2.372 | 28.45 | 0.684 |
| 180 | 0.755 | 1.034 | 3.570 | 45.88 | 2.500 | 33.17 | 0.681 |
| 200 | 0.723 | 1.034 | 3.700 | 49.50 | 2.590 | 35.82 | 0.680 |
| 250 | 0.653 | 1.043 | 3.977 | 59.00 | 2.794 | 42.80 | 0.677 |
| 300 | 0.596 | 1.047 | 4.290 | 69.00 | 2.970 | 49.90 | 0.674 |
| 350 | 0.549 | 1.055 | 4.570 | 79.00 | 3.15 | 57.50 | 0.676 |
| 400 | 0.508 | 1.060 | 4.850 | 90.10 | 3.29 | 64.9 | 0.678 |
| 500 | 0.450 | 1.072 | 5.400 | 111.2 | 3.62 | 80.4 | 0.687 |
| 600 | 0.400 | 1.088 | 5.820 | 136.6 | 3.92 | 98.1 | 0.699 |
| 800 | 0.325 | 1.114 | 6.680 | 189.0 | 4.45 | 137 | 0.713 |
| 1000 | 0.268 | 1.140 | 7.610 | 250.0 | 4.95 | 185 | 0.719 |
| 1200 | 0.238 | 1.164 | 8.450 | 314.0 | 5.39 | 232 | 0.724 |
| 1400 | 0.204 | 1.190 | 9.300 | 384.0 | 5.78 | 282 | 0.736 |
| 1600 | 0.182 | 1.220 | 10.110 | 459.0 | 6.16 | 338 | 0.740 |
| 1800 | 0.165 | 1.224 | 10.820 | 534.0 | 6.66 | 397 | 0.740 |

## 9.2 Appendix Table A.2: coefficient of thermal expansion of dry air

| Temperature | Density | | | | Specific weight | | Thermal expansion coefficient |
|---|---|---|---|---|---|---|---|
| [°C] | [kg/m$^3$] | [lb$_m$/ft$^3$] | [sl/ft$^3$*10$^{-3}$] | [lb$_m$/gal(US liq)] | [N/m$^3$] | [lb$_f$/ft$^3$] | [x10$^{-3}$ K$^{-1}$] |
| -75 | 1.783 | 0.1113 | 3.460 | 0.01488 | 17.49 | 0.11131 | 5.14 |
| -50 | 1.582 | 0.0988 | 3.070 | 0.01320 | 15.52 | 0.09878 | 4.55 |
| -25 | 1.422 | 0.0888 | 2.759 | 0.01187 | 13.94 | 0.08877 | 4.08 |
| -15 | 1.367 | 0.0853 | 2.652 | 0.01141 | 13.40 | 0.08532 | 3.92 |
| -10 | 1.341 | 0.0837 | 2.601 | 0.01119 | 13.15 | 0.08370 | 3.84 |
| -5 | 1.316 | 0.0821 | 2.553 | 0.01098 | 12.90 | 0.08214 | 3.76 |
| 0 | 1.292 | 0.0806 | 2.506 | 0.01078 | 12.67 | 0.08063 | 3.69 |
| 5 | 1.268 | 0.0792 | 2.461 | 0.01059 | 12.44 | 0.07919 | 3.62 |
| 10 | 1.246 | 0.0778 | 2.418 | 0.01040 | 12.22 | 0.07780 | 3.56 |
| 15 | 1.225 | 0.0765 | 2.376 | 0.01022 | 12.01 | 0.07645 | 3.50 |
| 20 | 1.204 | 0.0752 | 2.336 | 0.01005 | 11.81 | 0.07516 | 3.43 |
| 25 | 1.184 | 0.0739 | 2.297 | 0.00988 | 11.61 | 0.07390 | 3.38 |
| 30 | 1.164 | 0.0727 | 2.259 | 0.00972 | 11.42 | 0.07269 | 3.32 |
| 40 | 1.127 | 0.0704 | 2.188 | 0.00941 | 11.06 | 0.07039 | 3.21 |
| 50 | 1.093 | 0.0682 | 2.120 | 0.00912 | 10.72 | 0.06822 | 3.12 |
| 60 | 1.060 | 0.0662 | 2.057 | 0.00885 | 10.40 | 0.06619 | 3.02 |
| 80 | 1.000 | 0.0625 | 1.941 | 0.00835 | 9.81 | 0.06245 | 2.85 |
| 100 | 0.9467 | 0.0591 | 1.837 | 0.00790 | 9.28 | 0.05910 | 2.70 |
| 125 | 0.8868 | 0.0554 | 1.721 | 0.00740 | 8.70 | 0.05536 | 2.51 |
| 150 | 0.8338 | 0.0521 | 1.618 | 0.00696 | 8.18 | 0.05206 | 2.33 |
| 175 | 0.7868 | 0.0491 | 1.527 | 0.00657 | 7.72 | 0.04912 | 2.22 |
| 200 | 0.7451 | 0.0465 | 1.446 | 0.00622 | 7.31 | 0.04651 | 2.10 |
| 225 | 0.7078 | 0.0442 | 1.373 | 0.00591 | 6.94 | 0.04419 | 2.01 |
| 300 | 0.6168 | 0.0385 | 1.197 | 0.00515 | 6.05 | 0.03850 | 1.76 |
| 400 | 0.5238 | 0.0327 | 1.016 | 0.00437 | 5.14 | 0.03270 | 1.52 |
| 500 | 0.4567 | 0.0285 | 0.886 | 0.00381 | 4.48 | 0.02851 | 1.32 |
| 600 | 0.4043 | 0.0252 | 0.784 | 0.00337 | 3.96 | 0.02524 | 1.16 |
| 700 | 0.3626 | 0.0226 | 0.704 | 0.00303 | 3.56 | 0.02264 | 1.03 |
| 800 | 0.3289 | 0.0205 | 0.638 | 0.00274 | 3.23 | 0.02053 | 0.94 |
| 900 | 0.3009 | 0.0188 | 0.584 | 0.00251 | 2.95 | 0.01879 | 0.86 |
| 1000 | 0.2773 | 0.0173 | 0.538 | 0.00231 | 2.72 | 0.01731 | 0.80 |
| 1100 | 0.2571 | 0.0160 | 0.499 | 0.00215 | 2.52 | 0.01605 | 0.75 |

## 9.3 Appendix Table A.3: emissivity of the tube surface

| Surface Material | Emissivity Coefficient $\varepsilon$ |
|---|---|
| Aluminum Foil | 0.04 |
| Stainless Steel, weathered | 0.85 |
| Stainless Steel, polished | 0.075 |
| Stainless Steel, type 301 | 0.54 - 0.63 |
| Steel Galvanized Old | 0.88 |
| Steel Galvanized New | 0.23 |
| Iron polished | 0.14 - 0.38 |
| Iron, plate rusted red | 0.61 |
| Iron, dark gray surface | 0.31 |
| Iron, rough ingot | 0.87 - 0.95 |

## 9.4 Appendix Table A.4: Resistivity, Specific Heat and Thermal Conductivity as Function of Temperature

| **Stainless steel** *(19.11 % chromium; 8.14 % nickel; 0.60 % tungsten)* | | | | **Mild steel** *(0.23 % carbon)* | | | |
|---|---|---|---|---|---|---|---|
| Temperature (°C) | ρ (Ωm) × $10^{-6}$ | cγ (Ws/$m^3$ K) × $10^6$ | λ (W/mK) | Temperature (°C) | ρ (Ωm) × $10^{-6}$ | cγ (Ws/$m^3$ K) × $10^6$ | λ (W/mK) |
| 20 | 0.695 | 4.04 | 15.9 | 20 | 0.160 | 3.65 | 52.0 |
| 100 | 0.776 | 4.15 | 16.3 | 100 | 0.220 | 3.85 | 51.0 |
| 200 | 0.850 | 4.24 | 17.2 | 200 | 0.290 | 4.10 | 49.0 |
| 300 | 0.915 | 4.36 | 18.0 | 300 | 0.380 | 4.40 | 46.0 |
| 400 | 0.976 | 4.51 | 19.7 | 400 | 0.483 | 4.77 | 43.0 |
| 500 | 1.030 | 4.83 | 21.4 | 500 | 0.610 | 5.19 | 39.3 |
| 600 | 1.072 | 4.84 | 23.0 | 600 | 0.755 | 5.66 | 35.5 |
| 700 | 1.111 | 4.87 | 24.3 | 700 | 0.922 | 6.66 | 31.5 |
| 800 | 1.141 | 4.90 | 26.0 | 800 | 1.095 | 6.73 | 26.0 |
| 900 | 1.171 | 4.86 | 27.0 | 900 | 1.135 | 5.94 | 26.5 |
| 1000 | 1.196 | 4.87 | 28.0 | 1000 | 1.168 | 5.09 | 27.3 |
| 1100 | 1.220 | 4.93 | 29.0 | 1100 | 1.195 | 5.10 | 28.5 |
| 1200 | 1.241 | | 29.8 | 1200 | 1.22 | | 29.7 |
| 1300 | 1.257 | | 30.5 | 1300 | 1.24 | | 31.2 |
| | | | | 1400 | 1.26 | 5.08 | 32.8 |
| **Copper** | | | | **Aluminium** | | | |
| Temperature (°C) | ρ (Ωm) × $10^{-6}$ | cγ (Ws/$m^3$ K) × $10^6$ | λ (W/mK) | Temperature (°C) | ρ (Ωm) × $10^{-6}$ | cγ (Ws/$m^3$ K) × $10^6$ | λ (W/mK) |
| 20 | 0.017 | 3.39 | 395 | 20 | 0.0270 | 2.52 | 211 |
| 100 | 0.022 | 3.48 | 387 | 100 | 0.0364 | 2.59 | 219 |
| 200 | 0.033 | 3.57 | 380 | 200 | 0.0478 | 2.65 | 224 |
| 300 | 0.037 | 3.65 | 373 | 300 | 0.0599 | 2.71 | 223 |
| 400 | 0.044 | 3.72 | 366 | 400 | 0.073 | 2.78 | 216 |
| 500 | 0.052 | 3.77 | 360 | 500 | 0.087 | 2.84 | 209 |
| 600 | 0.060 | 3.82 | 353 | 600 | 0.104 | 2.89 | 200 |
| 700 | 0.068 | 3.87 | 347 | 700 | 0.210 | 2.51 | 92 |
| 800 | 0.077 | 3.92 | 341 | 800 | 0.225 | 2.52 | 88 |
| 900 | 0.086 | 3.96 | 335 | 900 | 0.235 | 2.54 | |
| 1000 | 0.097 | 3.99 | 330 | | | | |
| 1100 | 0.215 | 3.66 | 324 | | | | |
| 1200 | 0.222 | | 319 | | | | |
| 1300 | 0.228 | | 313 | | | | |

# 10 List of Figures

# 11 List of Tables

# 12 Acknowledgments

I would like to thank my parents and my brothers for the guidance and support that gave to me, without their help, I would not be the person I am today.

I would like specially to thank my older brother Eng. Alireza Alizadeh. He had been beside me in the whole journey of my master's and provided me with unlimited opportunities to grow myself as a better person.

I want to express my gratitude to my supervisor Prof. Roberto Faranda who always listened to my ideas and provided me with his deep insight and valuable comments. And hope in the future, there will be an opportunity to expand my knowledge and experience with him.

I want to thank Eng. Matteo Gianinetti has followed most of my activities, and it would be impossible to develop my work without his support. I will be grateful forever for all the experiences I have gained and learned working with him in Danieli.